The effect of probe length variation on Plasma parameters

Muhammad Mohsin Nawaz

Department of Physics

Quaid-E-Azam University

Islamabad, Pakistan

2023

The effect of probe length variation on Plasma parameters

This dissertation submitted to the Department of Physics, Quaid-i-Azam University, Islamabad, in the partial fulfillment of the requirement for the degree of

Master of Philosophy

In

Physics

By

Muhammad Mohsin Nawaz

Plasma Physics Laboratory
Department of Physics
Quaid-i-Azam University
Islamabad, Pakistan
2023

CERTIFICATE

This is to certify that the thesis entitled **"The effect of probe length variation on Plasma parameters."** by Muhammad Mohsin Nawaz submitted to Quaid-i-Azam University, Islamabad for the degree of Master of Philosophy (M.Phil.) in Physics is a record of Bonafede's research carried out by him in Experimental Plasma Physics Laboratory, under my supervision. I believe that this thesis fulfills part of the requirement for the award of Master of Philosophy. The result embodied in the thesis has not been submitted for the award of any other degree.

Chairman

Dr. Kashif Sabeeh
Professor
Department of Physics
Quaid-i-Azam University
Islamabad, Pakistan

Supervisor

Dr. Muhammad Shafiq
Professor
Department of Physics
Quaid-i-Azam University
Islamabad, Pakistan

Dedicated To

This work is humbly dedicated to our Holy Prophet HAZRAT MUHAMMAD (SALLALLAHU ALAYHI WA SALLAM) on whom ALLAH opened the doors of wisdom,

To my Hero my Father (Muhammad Nawaz) & My mother

My encouragement is from my teachers

My pride, my sisters

And Dr. Muhammad Sadiq.

Acknowledgments

First and foremost, I owe my deepest and heartfelt gratitude to **Almighty ALLAH**, for awarding me with the strength, physical and intellectual to achieve the challenging task of completing my M.Phil dissertation. I also offer my humblest gratefulness to **Holy Prophet HAZRAT MUHAMMAD (SALLALLAHU ALAYHI WA SALLAM)** who is the source of guidance and knowledge for the whole of humanity.

I am extremely grateful to my supervisor **Prof. Dr. Muhammad Shafiq** for his precious supervision and care. I cannot thank him in word's enough for putting his faith in me by giving me the liberty to carry out the research according to my desired path and believed process. His support empowered me to finish my research work in the shortest possible time.

I extend my heartiest appreciation to my father Muhammad Nawaz, my mother and my sisters for their consistent motivation in making me believe that 'I can do it' and my research might make a difference. My humblest and deepest gratitude for my parents, sisters and friends who always encouraged and helped me in every possible way. I cannot thank them enough for bearing my tough schedule during my M.Phil. studies. I owe all my academic success and achievements to my parents.

Special thanks to Dr. Zahid Iqbal Khattak. I appreciate his efforts to carry out my research work.

I am grateful to Dr. Muhammad Sadiq for his valuable guidance. I cannot thank him sufficient for pushing his trust in me by giving me the right to carry out the research according to my preferred track and understood development. His support enabled me to finish my research work in the possible duration.

I would like to thank all the faculty members at the department of Physics at Quaid-i-Azam University who had taught me and helped me in my M.Phil. research work. Moreover, I cannot forget the mention Mr. M. Sadiq, Mr. M.Asad-Ullah, Mr. M.Yasin and Mr. Aijaz who were great help in all administrative matters during my M.Phil. dissertation.

I owe sincere thanks to senior PhD scholars especially Mr. Habib-ur-Rehman, Mr. M. Imran Bashir and Mr. M. Asghar, as well as Lab fellows Ahsan Ali, Shehbaz Hassan and friends Ali Abbas, M. Munawar Ali, Kishwar Ali, and my juniors Usman-ul-Haq, and Bilal Anjum.

I would like to thank my all class fellows Mohsin Naeem, Mohsin Raza, Muzammil Ahmad, Farwa Naz, Amna Huq, Wajahat Hussain and Maaz Ahmad for their support and cooperation during my study.

I am grateful to all my friends and cousins Raess Ali Sher, Sheryar Ali Sher, Mubashir-ul-Hassan, Asad Ali Abbas, Abdul Rahman Arshad, Usama Faisal, Muhammad Junaid, Hashim Bilal, Umair Nawaz and Shoaib Khan for their cooperation.

I would like to thank my uncle Muhammad Nawaz and Zafar Iqbal. I owe sincere thanks to my sisters Muqaddas Nawaz, Esha Nawaz, Rida Nawaz, Kinza Nawaz, Kanwal Aziz, Ghazal Mushtaq, Tahira Noor and my family friends Ramal Ahmad, Andleeb Kanwal, Maria Gul, and Kinza Saleem. All these mentioned are my supporters and my beloved family members.

Muhammad Mohsin Nawaz

Table of Contents

List of Figure

Abstract

This study examines the impact of varying probe length on the measurement of Argon plasma parameters like electron density (n_e), electron temperature (T_e), plasma potential (v_p), and electron energy probability function (EEFP). Argon plasma is generated in MaPE-ICP system for investigating the plasma parameters like electron density (n_e), electron temperature (T_e), plasma potential (v_p), and electron energy probability function (EEFP) by employing Langmuir probe with length ranging from 5mm to 10mm. The experiment is conducted under varying RF power (10watt, 30watt, 50watt, 70watt, and 100watt) with constant pressures (1 Pa, 5 Pa and 10 Pa) respectively it is observed that electron density (n_e) shows increasing trend as the probe length increases at constant RF power and pressure. It is also observed that electron temperature (T_e) initially rises with probe length but gradually decreases beyond 6mm. Plasma potential (v_p) decreases with probe length and the highest potential is observed at minimum RF power. Electron Energy Probability Function (EEPF) exhibits a declining trend with increasing energy.

By using the Langmuir Probe as primary diagnostic tool, this research highlights the involved relationship between probe length, RF power, and plasma parameters. The results, underscore the significance of considering probe characteristics in plasma diagnostics.

CHAPTER 01

INTRODUCTION TO PLASMA

1.1 Introduction

According to the ancient Greek philosopher Aristotle, the four states of matter are "earth, water, air, and fire" [1]. Currently, the three states of matter are solids, liquids, and gases. Plasma is the fourth state of matter. According to some approximations, plasma makes up almost 99% of all observable matter in the cosmos. In simple terms, plasma is found in the magnetic fields around the sun (called magnetospheres) and the outer layers of some planets, moons, and comets (called ionospheres). Although the given estimate might not be perfectly precise, it is definitely true to some degree.

An ionized gas is a plasma. A solid becomes a liquid when heated to a temperature, similar to this gas is created when a liquid is heated to a point where surface atoms evaporate more quickly than they condense. The "fourth state of matter," plasma, is created when a gas is heated to the point that atoms clash and lose their electrons. So, this terminology plays a big role in determining when the change from a "very weakly ionized gas" to a "plasma" takes place. The fact that an ionized gas has different characteristics is important. In plasma, ion-electron charge separation generates electric fields, while fluxes of charged particles generate currents and magnetic fields. These fields produce "activity at a distance" and a variety of phenomena that are astonishingly complex, extremely useful, and occasionally extremely beautiful [2].

The simplest explanation of plasma is “a disorganized combination of neutral particles, ions, and electrons with a lot of microscopic activity” [3].

It is difficult to describe the transformation of the gaseous state of matter into plasma because as a fundamental state, the plasma cannot be fully explained. The more useful description of plasma is that:

“A collection of particles namely neutrals, electrons and ions which moves randomly and plasma behave like conductor due to presence of these charged particles”

When all ions in a gas are present to some extent, no ionized gas can be referred to as plasma. This results in the basic definition of plasma, which is: "A plasma is a quasi-neutral gas containing charged particles and neutral particles that show collective behavior"[4].

The plasma state is a mixture of ionized gas and Quasi-neutral containing an equal number of free electrons, positive ions, and many neutral atoms and molecules that show collective behavior. Any ionized gas cannot be treated as plasma, Quasi-neutrality and collective behavior are fundamental features of plasma. There are three conditions in terms of plasma parameters for an ionized gas to be plasma:

i. $\lambda_D << L$ i.e. The Length of Debye shielding must be smaller than the dimension L of the system.
ii. $N_D >>> 1$ i.e. Number of particles in the Debye sphere must be also much greater than one.
iii. $\omega\tau > 1$ i.e. the mean time between collisions per plasma oscillation must be greater than one.

1.1.1 Quasi-Neutral

Quasi neutrality is attributed to the balance of charged species that according to the plasma it is probable to approximate the total number of negative charges are equivalent to the total quantity of positively charged species while the plasma is not to be considered as neutral which the stimulating electromagnetic induction is may be ignored. Hence plasma is whole neutral so; $n \cong n_e \cong n_i$.

This characteristic of plasma is known as quasi-neutral where 'n_e' is the number of electrons and 'n_i' is the number of ions.

1.1.2 Collective Behavior

The difference between a neutral gas and plasma can be explained with the understanding of particle interactions. From the kinetic theory of gases, there is no net electromagnetic force on the gas particles. The gas particles carry no net charge are electrically neutral and can interact only during collisions. The short-range Vander Waals forces in a neutral gas decrease with inter particle spacing as r^{-6} while in the plasma, there are free charged carriers (positive ions and electrons) and they interact by the coulomb electric force (The long-range) decreases with interparticle distance as r^{-2}[5]. When charge particles move in the plasma, they create an electric field as well as a current and magnetic field. The electric and magnetic fields affect the motion of another charged particle. Each plasma particle interacts with many other particles and plasma exhibits simultaneous as well as cooperative responses of many particles known as collective behavior. Plasma shows the collective

response to external perturbations. The response to perturbation of electromagnetic field, Debye shielding, and wave processes are best examples of Collective behavior [6].

Figure 1.1 illustrates the deviation of the Coulomb force at a distance of "**r**" and dimensions of $\frac{\mathbf{1}}{\boldsymbol{r^2}}$ between two plasma volume elements A and B.

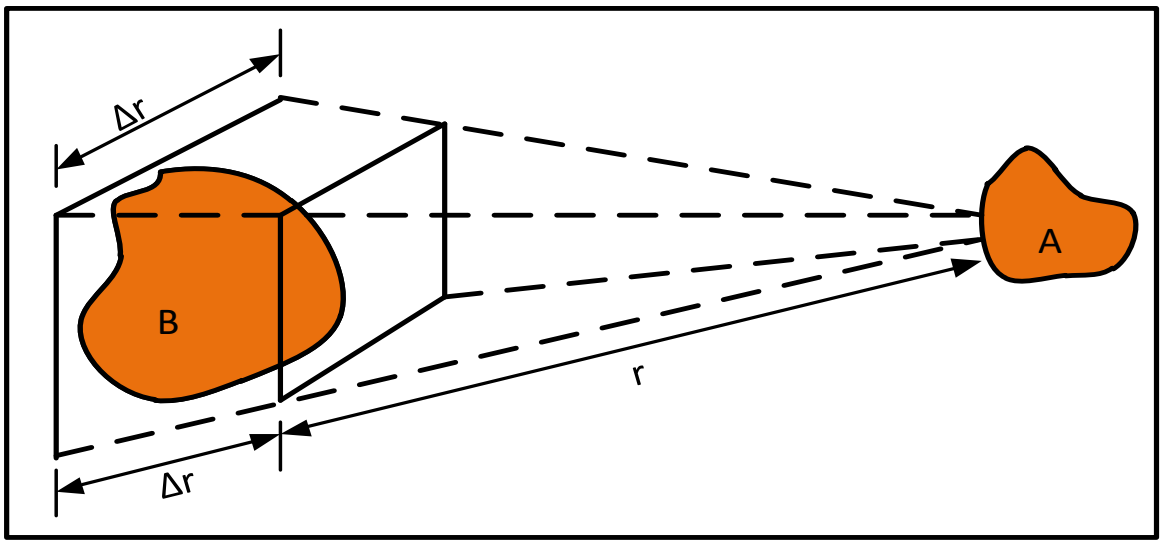

Figure 1. 1: Diagram of long-range coulombic forces in plasma [4].

Assuming a solid angle (where $\frac{\Delta r}{r}$ = constant), the amount of plasma in B that affects A increases a lot as r^3. This means that even when they are far apart, plasma elements push and pull each other. The reason for this is a special kind of force called long-ranged Coulomb force, and it makes the study of plasma physics very interesting. The most fascinating findings are about "collision less" plasmas. In these cases, the long-range electromagnetic forces are much stronger than the forces from regular local collisions, so we can ignore those. When we say "collective behavior," we mean motions that don't just depend on what's happening nearby but also on what's going on in distant parts of the plasma.

1.2 History of Plasma

It appears that the term "plasma" is confusing. Its origins are Greek, and its meaning is "jelly" or "anything molded or manufactured." Plasma has collective behavior, which makes it less likely to accept outside forces and more likely to act independently.

In 1927, Irving Langmuir was the first scientist to implement the term "plasma" to refer the plasma as an ionized gas. He was comparing the way an electrified fluid conveys electrons and ions, to how blood plasma carries red and white blood cells.

In order to discover, Langmuir investigated the physics and chemistry of tungsten-filament light bulbs. During this investigation, he established a theory of plasma sheaths and the boundary layers between ionized plasma and solid surfaces. Langmuir waves are a phrase used to describe the sections of a plasma discharge tube that display periodic changes in electron density. This was where plasma physics began. According to Langmuir's research, the majority of plasma processing methods used today to create integrated circuits have a theoretical foundation. Plasma research increased in numerous directions following Langmuir's work.

Hannes Alfven created magneto-hydrodynamics which plasma treats basically as a conducting fluid. A wide range of astrophysical phenomena, including the sunspot, solar flares, solar wind, and star formation, have all been studied using this theory. The supersonic solar wind idea and the spiral structure of the solar magnetic field in the outer solar system were developed by an American solar astronomer in 1950. Parker put out a theory in 1987 that the small flames observed all over the sun's surface could heat the solar corona.

The development of the hydrogen bomb in 1952 sparked a lot of curiosity in the possibility of using controlled thermonuclear fusion as a future energy source. While thermonuclear fusion research was formally acknowledged in 1958. This year, theoretical plasma physics became the first scientific field to be rigorously grounded in mathematics.

James A. Van Allen used information sent to him by the United States in 1958 to find the Van Allen radiation belts encircling the planet. The field of space plasma physics was introduced with the launch of the first systematic satellite exploration of the Earth's magnetosphere. Finally, the field of laser-plasma physics was made possible in 1960 by the development of the laser. This new finding states that when a laser beam hits a solid target, the material is quickly ablated and a plasma is formed at the beam-target boundary.

1.3 Occurrence of plasma

Dark energy makes up 69% of the universe mass, whereas dark matter makes up 27% of it. All of this is visible in the sky and is made up of ordinary matter that is in a plasma state. Plasma is an ionized gas in which at least one of an atom electrons has been stripped away, leaving a positively charged nucleus known as an ion. Blood plasma is not to be confused with plasma because it is not an ionized gas.

While 99% of the universe stuff is in a plasma state, we only occupy 1% of it, which is where plasma does not normally form. There are only a few examples of plasma on Earth,

including the pixels of plasma television, the flash of a lightning bolt, the conducting gas within a fluorescent tube or neon sign, a small amount of ionization in a rocket exhaust, and the gentle glow of the Aurora Borealis.

Plasma normally only exists in a vacuum. In contrast, air will cool the plasma, which will cause the ions and electrons to unite once more to form regular neutral atoms. Within the lab, a pump is required to remove air from the chamber to create the vacuum. Vacuum is important for the generation of plasma in the lab.

i- Plasma in space

Plasma is also present in space such as in, the sun, coronas, solar winds, star nurseries, and interstellar nebulae. It is also present in the magnetic fields of many planets. The sun is a 1.5 million km ball of plasma that is 99.85% plasma and heated by nuclear fusion. Space is not a void that is empty. Plasma makes up 99.9% of the universe.

ii- Terrestrial plasma

When the temperature of the fire exceeds 1500 ℃, plasma is also present. Thus, plasma can also be found in sprites, polar aurora, polar wind, the magnetosphere, the ionosphere, the plasma sphere, and lightning.

iii- Artificial plasma

TV screens, neon signs, the area in front of a spacecraft's heat shield during re-entry into the atmosphere, within a corona discharge ozone generator, fusion energy research, the electric area in an arc lamp, an arc welder, or plasma torch, an arc created by a tesla coil, laser-made plasma, static electric spark, capacitive coupled plasma (CCP), dielectric barrier discharges (DBD), and in fusion test reactors (TNFP).

1.4 Generation of Plasma

Processes of ionizations, excitation processes, and Electron loss mechanisms are the fundamental processes in plasma. Processes of ionization consist of the direct impact of the electron, stepwise ionization, a beam of high-energy electrons, photoionization, and ionization of surface atoms it is also known as electron emission and penning ionization. While excitation processes include electron impact excitation, charge transfer excitation, penning excitation, and ion-electron recombination. The electron-ion recombination

process and the electron attachment process make up the electron-loss mechanism. The subsequent discussion covers each of these key procedures.

1.4.1 Processes of Ionization

Neutral atoms or molecules can become electrically charged by gaining or losing electrons during the ionization process. Plasma ionization is crucial because it influences, how plasma is reactive. The following categories can be used to classify it [7].

1.4.1.1 Direct Electron Impact Ionization

Direct ionization by electron impact is the first group process of ionization. In this group, when high-energy electrons directly connect with the electron of the outermost shell of neutral atoms or molecules they ionize it. It happens when the electron's energy is greater than the neutral particle's ionization potential. The amount of excitation of neutral species is mostly typical when the electric field energies are large during cold or non-thermal discharge. For diatomic molecule (PQ), it can be written as follows [8];

$$\begin{aligned} e + PQ &\rightarrow PQ^{+} + e + e \\ e + PQ &\rightarrow P + Q^{+} + e + e \\ e + PQ &\rightarrow P + Q^{*} + e + e \end{aligned} \qquad (1.1)$$

In the above equations, P represents the neutral atom.

Q^{+} represents the ionized atom.

PQ^{+} shows the ionized molecule.

Q^{*} stands for excited atom.

1.4.1.2 Stepwise Ionization

This is the second group of the ionization process. For the ionization of neutral particles, we required a higher ionization potential than the electron average energy in plasma. In this case, direct ionization of electron impact occurred because of high energy electrons towards the end of the distribution function. [9]. In metastable atoms, ionization probability is relatively greater because the ionization potential is rather a few times smaller than the comparison to the ground state atoms [10]. Ionization of excited atoms occurs when excited atoms interact with low-energy electronic particles. This is the result of an electron impact progressive ionization [11]. The degree of ionization (ratio of electron to neutral number

densities) and the concentration of highly excited neutral species must be relatively high in order for this set of ionization processes to of normal or energy-intense discharge [10].

1.4.1.3 Ionization by collision

The third category of ionization processes involves ionization caused by the collision of heavy particles, which can occur during ion-atomic or ion-molecular collisions. Electrically or vibrational stimulated species collide when the combined energy of their collision partners exceeds the ionization potential. Ionization and other processes can be aided by the chemical energy of colliding neutral particles. This procedure is also known as the associative ionization method [10].

1.4.1.4 Ionization by high-energy electron beam

Plasma can be generated by high-energy electron beams. In this case, atmospheric pressure ionization is more homogeneous and produces uniform non-thermal plasma. Electron beams work well together when the electric field is stable, and because of this field, they create ionization and use up energy. The electron energies in this system range from$\sim 50\ keV\ to\ \sim 2\ MeV$, and the energy losses of the electron beam through the air due to atmospheric pressure are roughly$\sim 1\ MeV/m$. Because of this, the process of producing plasma in large quantities requires beams with high energy [10].

1.4.1.5 Photoionization processes

In this process, incoming photons whose energy is equivalent to or greater than the ionization potential of the absorbing atom are absorbed, causing ionization to occur. The extra photon energy is converted into the kinetic energy of the newly generated electron-ion pair. X-rays and gamma rays, which have considerably shorter wavelengths, can also ionize materials. For instance, the ionosphere of the Earth is a naturally photo-ionized plasma. In thermal plasma and some non-thermal discharge propagation, the photoionization process is essential.
The reaction can be written as [10].

$$h\nu + P \rightarrow P^{+} + e \qquad (1.2)$$

Under ideal conditions due to the limited number of energetic photons, photoionization influence on plasma is not very large [7].

1.4.2 Electron emission

This is the fifth group of ionization processes. When the surface is heated, the interaction between high-energy electrons, ions, and photons with surface atoms causes the ejection of electrons from the atom. This phenomenon is called surface ionization or electron emission [7].

1.4.2.1 Associative and Penning Ionization

A Dutch scientist named Frans Michael Penning first discussed this process, so it is named "Penning Ionization."[12]. The molecular ion *AB* and the molecules AB* went through several vibrational states as the process progressed.

$$A^* + B \rightarrow AB^+ + e \qquad \text{(Associative Ionization)} \qquad (1.3)$$

The energy of the electron in the final state should be less than the energy of the electron in the initial state for this process to occur. This process is effective for excited states. In the case of associative ionization, it occurs through the attractive term AB* with a cross-section approximately equal to the kinetic gas cross-section [13].

The penning ionization process is the name given to the ionization act that results when the electron therefore excitation energy of metastable atom A* surpasses the ionization potential of another atom B. The process can have a very broad cross-section and typically involves the intermediate production of an unstable quasi-molecule. Following is an expression for the penning ionization process [14].

$$A^* + B \rightarrow A + B^+ + e \qquad \text{(Penning Ionization of Atoms)} \qquad (1.4)$$

$$A^* + B_2 \rightarrow B_2^+ + A + e \qquad \text{(Penning Ionization of Molecules)} \qquad (1.5)$$

1.4.3 Excitation Process

During this process, they are responsible for generating the electron components of the plasma and offering a basic comprehension of the radiation produced by this system. The primary mechanism for generating excited atoms in plasma is through collisions between atoms and electrons. The following can be used to describe this procedure [15]:

$$e + A \rightarrow A^* + e \qquad (1.6)$$

1.4.3.1 Electron-Loss Mechanism

The "Electron-Loss Mechanism" refers to the process by which electrons are removed or lost from a system, material, or, in specific contexts like plasma, describing how electrons are depleted from the overall electron population. In simple terms, when things get turned into plasma, we believe that electrons and positive ions are the reasons. We're looking into how electrons are lost in this process, and it involves studying the basics of plasma degeneracy. The whole investigation checks how charged particles balance out and how much plasma is there. The electron loss mechanism covers various ways electrons can be lost.

1.4.3.2 Electron-ion recombination process

The electron-ion recombination process is when an ion grabs a free electron after a collision, and they both become stable. A significant amount of energy is produced during this process of electrons being lost, and this energy is used in many other processes, like dissociation. The fastest way to neutralize electrons when molecular ions are around or in molecular gases is through dissociative electron-ion recombination [16].

$$e + AB^{+} \rightarrow (AB)^{*} \rightarrow A + B^{*} \tag{1.7}$$

The recombination energy is typically used in two ways during this process: by separating the molecular ion and exciting the resulting products. The loss of an electron can happen in the three-body electron-ion recombination, either during interactions with atomic ions or when molecular ions are not present [17].

$$e + e + A^{+} \rightarrow A^{*} + e \tag{1.8}$$

In this situation, a third-body partner is like a free electron's energy that joins in the recombination. Heavy particles like ions and neutrals can't quickly absorb the recombination energy into their energy and aren't useful as third-body partners at this moment. The final phase is radiative electron-ion recombination, where the recombination energy turns into radiation or the electron is lost [18].

$$e + A^{+} \rightarrow A^{*} \rightarrow A + h\nu \tag{1.9}$$

Only three-body recombination can compete with this process' low process efficiency and low plasma density, which are both critical factors in low-temp plasma dynamics.

1.4.3.3 Electron attaches and de-attachment process

The process of electron attachment happens when an electron joins with a neutral, creating a negative ion. This is essential for breaking apart electronegative molecules, various chemical reactions in plasma, and activities where plasma acts as a catalyst, as well as serving as a way for electrons to be lost. The rate at which this dissociative attachment occurs is directly linked to the electron density, following the first-order relationship with the concentration of electrons [19].

$$e + AB \rightarrow (AB^{-})^{*} \rightarrow A + B^{-} \qquad (1.10)$$

Here $(AB^{-})^{*}$ is the auto-ionization state or excited state while $(A+B^{-})$ is the automated attachment or dissociation state. When an electron interacts with the heavy particles one of them has positive electron affinity then the electron attachment arises with the positive electron affinity molecules [20].

1.5 Plasma Parameters

Plasma can be examined in terms of many parameters. As the plasma density, electron density, electron temperature, plasma potential and electron energy distribution function (EEPF) are explained in this part.

1.5.1 Plasma density

The discussion often revolves around the percentage of ionized gas in a given volume as it relates to gas particle absorption in that volume. Material efficiency in each plasma process closely depends on the density of charged particles. Plasma density is a critical parameter in many material processing applications. Charged particles, such as ions and electrons, experience a force from the applied electric field, resulting in their acceleration and absorption of energy. Electrons, with their light mass, can be easily accelerated by the external electric field, allowing them to absorb a significant amount of energy. When these energetic electrons interact with neutral particles, excitation and ionization processes occur. Enhancing the electron density intensifies the efficiency of these reactions.

To boost plasma reactions, we need to increase the plasma density, but if we push it too much, our components might get extremely heated. Changes in plasma density and its characteristics depend on this density level. The majority of the plasma used in the surface modification business is cold plasma, which is formed at lower temperatures and has a very low density. While the plasma density in normal plasma is typically less than 1%, or about

100 million electrons per cubic centimeter, the plasma density in hot plasma is quite high, or around one trillion electrons per cubic centimeter.

1.5.2 Electron Density(n_e)

Electron density has a key role in the material processing application of plasma. Plasma density is necessary for better knowledge of the gas discharge. Electron density is a very important parameter in the plasma. Electrons take part in the excitation ionization and dissociation process and are responsible for the chemical reactions in the plasma. The Electron density is obtained by means of the energy distribution function in the Langmuir probe method:

$$n_e = \int_0^\infty f(\epsilon) d\epsilon \qquad (1.11)$$

The Debye length and Quasi-neutrality are described by electron number density.

1.5.3 Electron Temperature (T_e)

The average kinetic energy of free electrons in the plasma is also known as electron temperature. In high-density plasma electron temperature is one of the most crucial variable in low-pressure. The fluxes and energy distribution of charged particles are obtained with the help of electron temperature. Electrons control the chemical events taking place inside the plasma in addition to being engaged in the dissociation, excitation, and ionization of atoms or molecules. Electron temperature (T_e) can be measured by the electrostatic Langmuir Probe [20].

In low-temperature plasma, the temperature of heavy particles like ions is commonly very small as compared to the light particles as electrons. So the involvement of ions to increase the chemical reaction is very small [21]. At thermodynamics equilibrium electron temperature (T_e) has a Maxwellian velocity distribution function which is determined by the average translational kinetic energy of free electron in plasma. Maxwellian distribution is based on the condition of thermodynamics equilibrium (T_e=T_g).

$$< \varepsilon >= \frac{3}{2} K_B T_e \qquad (1.12)$$

In a non-thermal plasma, the electron temperature is dictated by the mean energy of the non-Maxwellian distribution function [22].

$$T_e = \frac{3}{2} < \varepsilon > \quad (1.13)$$

or

$$T_e = \frac{3}{2} \int_0^\infty \epsilon f(\epsilon) d\epsilon \quad (1.14)$$

Here in the above equation $f(\epsilon)$ is a non-Maxwellian energy distribution function.

1.5.4 Plasma potential(V_p)

The electric potential at which the net charge density in the plasma becomes zero is called plasma potential. In simpler terms, it is the potential at which electrons and ions collectively achieve a balanced state, leading to a state of quasi-neutrality. In a plasma, positive ions and negative electrons move around. This movement creates the plasma potential because these charged particles make an electric field. In a stable plasma, positive and negative charges are about the same, making it quasi-neutral. The plasma potential is where the electric field from these charges balances out. Charged particles in a plasma feel the electric field from the plasma potential, making electrons and ions move and affecting the overall plasma. When the charged particles' movement calms down, and there's no net charge, the system is in balance, and the potential at this point is the plasma potential.

Plasma potential influences interactions between the plasma and surrounding materials. Controlling the potential is important in processes like plasma etching or deposition used in semiconductor manufacturing. The potential affects the energy distribution of charged particles. Knowledge of plasma potential is vital for optimizing conditions in plasma devices where specific energy levels are desired.

1.5.5 Electron Energy Distribution Function (EEDF)

Statistical mechanics focuses on understanding the most likely behavior of a system with many particles as a whole, rather than concentrating on the actions of individual particles. The distribution provides information about the likelihood of a particle being in a state with a certain energy (ϵ). With this distribution knowledge, various useful calculations can be made, such as electron mobility, diffusivity, reaction rates, and more [23].

In a statistical system, the particles are represented by a distribution function $(\vec{r}, \vec{v}, t)$, which tells us about the number of electrons in the velocity space per unit volume. Figure 1.2 shows sketch of velocity in Cartesian coordinates system.

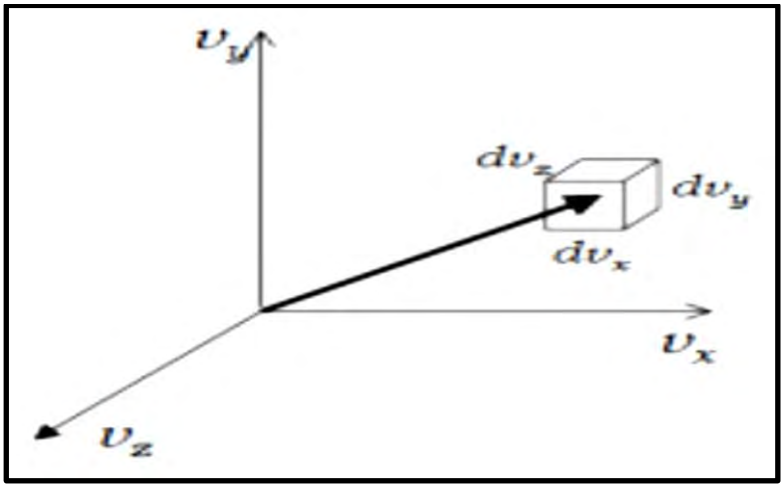

Figure 1. 2: Sketch of velocity in Cartesian coordinates system [23].

$$f(x, y, z, v_x, v_y, v_z)dv_x dv_y dv_z$$

$$dv_x dv_y dv_z = d^3v$$

The electron density is obtained at any time t and position $\vec{r}$:

$$\mathrm{n}(\vec{\mathrm{r}},\ \mathrm{t}) = \int_{-\infty}^{\infty} \mathrm{f}(\vec{\mathrm{r}}, \vec{\mathrm{v}}, \mathrm{t})\mathrm{d}^3\mathrm{v} \qquad (1.15)$$

Figure 1.3 shows sketch of Velocity components from Cartesian to spherical coordinates hence in spherical coordinates:

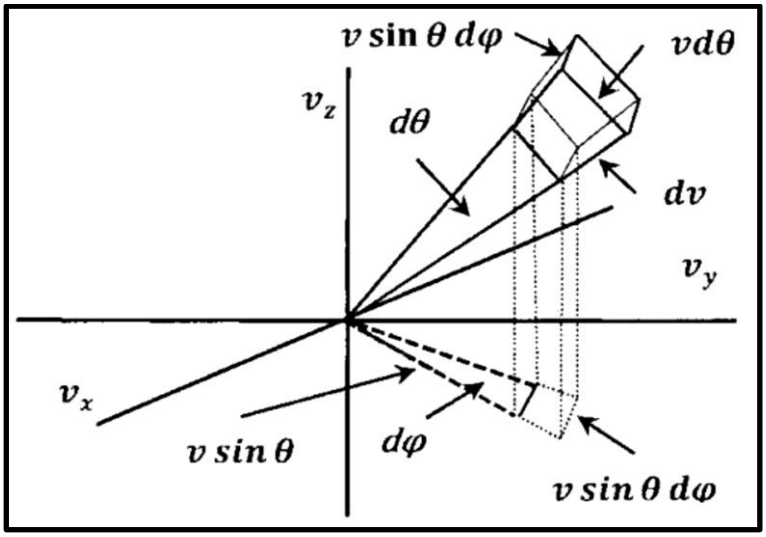

Figure 1. 3: Sketch of Velocity components from Cartesian to spherical coordinates [23].

The volume element is $d^3v = v^2 \sin\theta d\theta d\varphi dv$ and one can calculate the relation:

$$\int_0^{\pi} \sin\theta \int_0^{2\pi} \mathrm{d}\varphi \int_0^{\infty} \mathrm{v}^2 \mathrm{f}(\mathrm{r}, \mathrm{v}, \mathrm{t})\mathrm{dv} = 4\pi \int_0^{\infty} \mathrm{v}^2 \mathrm{f}(\mathrm{r}, \mathrm{v}, \mathrm{t})\mathrm{dv} \qquad (1.16)$$

A relation between electron energy distribution function (EEDF) and electron velocity distribution function (EVDF) is:

$$f_E(\epsilon)d\epsilon = 4\pi v^2 f_v(\epsilon)dv \quad (1.17)$$

Where $\epsilon = \frac{1}{2}m_e v^2$

At a state of thermal equilibrium, the classical Maxwellian Boltzmann distribution is the most expected pattern. In a gas at thermal equilibrium, there are particles with different speeds. In an isotropic plasma, the electron velocities are expected to follow the Maxwellian distribution. The impacts of electron interaction are explained through the energy distribution function of electrons. The velocity distribution function for electrons, also known as EVDF, is described by the Maxwell-Boltzmann distribution [4].

$$f(v) = n_e \left(\frac{m_e}{2\pi K T_e}\right)^{3/2} \exp\left(-\frac{m_e v^2}{2K T_e}\right) \quad (1.18)$$

The Maxwellian distribution function (EEDF) is:

$$f(\epsilon) = n_e \frac{2}{\sqrt{\pi}} \left(\frac{1}{K_B T}\right)^{3/2} \epsilon^{1/2} \exp\left(-\frac{\epsilon}{K_B T}\right) \quad (1.19)$$

Maxwell-Boltzmann theory supposes that the energy distribution for all species (electrons, ions, and neutral atoms) follows a Maxwellian pattern at equilibrium temperature. When there's quasi-neutrality($n_e \approx n_i$), it ensures an electric field $\vec{E} = 0$ within the plasma bulk, and the plasma potential ($\emptyset_r \cong \emptyset_0$) remains reliable across space. As a result, in a Maxwellian plasma, no current flow or particle transport occurs, maintaining uniformity.

In low-pressure situations with non-LTE plasma, the distribution isn't Maxwellian. Here, the Druyesteyn method helps find the energy distribution (EEDF) [24]. It's specifically used to figure out the EEDF for electrons in isotropic plasma.

$$f(\in) = \frac{1}{e^2 A_p}\sqrt{\left(\frac{8 m_e V}{e}\right)}\frac{d^2 I}{dV'^2} \quad (1.20)$$

The low pressure (non-LTE plasma) show non-Maxwellian nature. In this case, energy distribution (EEDF) for electron is related to the energy probability function (EEPF).

$$f(\in) = \in^{-\frac{1}{2}} f(\in) \quad (1.21)$$

1.5.6 Excitation Temperature

Excitation temperature is one of the parameters that is also determined by emission spectroscopy. In plasma, the term excitation temperature (T_{exc}) is used for the energy of excited species. This temperature (T_{exc}) explains the distribution of excited energy levels using the Boltzmann distribution [25].

$$\ln\left[\frac{\varepsilon_{ji}\lambda_{ji}}{A_{ji}g_j}\right] = -\frac{E_j}{K_B T_e} + C \qquad (1.22)$$

In thermal plasma, the process of excitation or de-excitation is dominant due to collisions as compared to radiative interactions, and so in such plasma excitation temperature and electron temperature is assumed to be equivalent ($T_{exc} \approx T_e$) In thermal plasma, density is very high ($\sim 10^{16} cm^{-3}$) [21]. While in the laboratories local thermodynamics is difficult to achieve, one can assume excitation temperature calculated from the emission intensities is equal to the electron temperature and gas temperature [26].

1.6 Types of Plasma

Plasma comes in two different varieties. The terms "hot plasma" and "cold plasma" refer to different types of plasma, respectively. These plasma kinds are determined by the particle temperature. Both types of plasma are crucial to plasma physics as well as other scientific disciplines.

1.6.1 Hot plasma or LTE (Local Thermodynamic Equilibrium)

This type of plasma is also known as local thermodynamics equilibrium (LTE).This type of plasma is nearly the same as the thermodynamics equilibrium model except that the radiation process is not in detail balanced [19]. The collisional interactions lead to atomic transitions and chemical reactions. While the radioactive process has no importance because the radiation field did not follow the Planck distribution [27]. In other words, the plasma in which each temperature except the temperature of radiation (T_r)is equal in a small volume of plasma and this is also known as thermal plasma. The following mainly two conditions are existing for this form of plasma.

- The heavy particles in the plasma that possess high energy at high-temperature ($10^6 \sim 10^8$ K).
- Pressure will be atmospheric even at 6000 K temperature.

When the pressure in plasma increases, ions and electrons present in plasma will collide normally due to the less mean distance between them. When atmospheric pressure is attended inside the system the ions and the electrons will try to gain the same thermodynamic equilibrium [28]. LTE plasma (containing energetic heavy particles) is created to make a managed thermonuclear fusion process.

In the laboratory plasma that has high density and low temperature is described by the LTE model in which the collisional processes are dominant over the radiative processes without affecting the population distribution. The collisional process relies on the specific conditions in the local plasma, while the radiative process is non-local, depending on the population distribution of other spatial points for the LTE model to accurately depict a plasma [29].

$$n_e(cm^{-3}) \geq 1.6\times10^{12}\, T_e^{1/2} \Delta E^3 \qquad (1.23)$$

In the above equation, *it* is the small electron density that is required to sustain the LTE state via collisions to compete with the simultaneously radiative processes. ΔE is the energy difference in eV between the radiative states. T_e is the electron temperature in eV. In radiative plasma, T_g and T_e are considered the same.

1.6.2 Cold Plasma or Non-LTE (Non-Local Thermodynamic Equilibrium)

A type of plasma in which electrons and ions cannot gain thermodynamic equilibrium. In this type of plasma, the electron temperature (T_e) is very high as compared to the ion temperature (T_i) ($i.e: T_e >> T_i$). Moreover, in this type of plasma ion temperature (T_i) is higher than the gas temperature (T_g) so the gas temperature (T_g) is higher than the excitation temperature (T_{exc}) (i.e: $T_e > T_i > T_g > T_{exc}$) [30].

To put it another way, the thermal motion of the ions in this kind of plasma can be disregarded. As a result, there is no pressure force, magnetic force can be ignored, and only electric force is considered to act on the particles [31]. In this type of plasma gas temperature is noticed as low as room temperature and the temperature of electrons reaches up to 10^5K.

Physical and chemical reactions can occur in this plasma at very low temperatures. Therefore, cold plasma qualities have been created and improved for this purpose. Although the rate of de-excitation by electron collision is lower than the rate of excitation

caused by the electron, the de-radiator excitation's power is high. The electron thermal velocity is greater than the ions in the non-LTE plasma.

1.7 Generation of Low-Temperature Discharges

When we apply external power to a low-pressure gas, it forms a type of plasma known as low-temperature plasma. Radiofrequency (RF), direct current discharges (DC), and microwaves (MW) are some of the numerous ways that plasma is produced. Mostly these kinds of plasma can be generated with the help of modern techniques by passing current across the gas and so it is also known as gas discharges. These techniques are important because they are applied in the manufacturing of materials and for industrial applications**.**

1.7.1 Radio Frequency (RF) Discharges

Instead of using real currents to transfer signals to the plasma in this type of discharge, the power source depends on displacement current. In simple terms, displacement current is a method of communication that does not involve the actual flow of electricity. Inside the plasma displacement current is created by RF power which delivers energy to the plasma [32]. In laboratory and industrial scale devices are not easy for the generation of stable plasma and it becomes a challenging task in many modern applications. Due to big achievements in technologies of science and the semiconductor industry motivated researchers to look for a better option than the conventional DC charges due to the limitations of DC discharges. Radio-frequency discharges work well as an alternative. The use of radio frequency is more significant than the use of DC discharges. One of the vital applications is the etching and deposition of a thin solid layer on the material that is placed on the electrode. When an insulator layer has to be treated, the DC charges plasma cannot be maintained for a long period under such conditions, so the RF plasma becomes essential [33, 34].

The RF power sustains the plasma in a stable state and the gas pressure used in this type of device is normally below the atmospheric pressure. In a few cases, atmospheric pressure can be utilized and these discharges can run in the frequency range of 1 to 100 MHz [30]. The frequency of the RF power supply for lab and commercial plasma systems is set by international telecommunication authorities. They picked frequencies that weren't used by civilians or the military to avoid messing with radio communication. Such high-frequency power in the generator causes much noise in nearby areas of the laboratory. A 13.56 MHz frequency was used for the production of cold plasma and secured to moderate the noise

problem. If someone wants to perform the experiments with a frequency other than the fixed value (13.56 MHz) then proper protection for the experiment should be used. 13.56 MHz power supplies are reasonably priced and well-developed, and RF power supply manufacturers have various products at this frequency.

In RF discharges two conditions govern the operating system [35].

The first condition is the low-frequency region ($\omega_{pe} \gg \omega_{pi} \gg \omega_{rf}$) in which both ions and electrons oscillate with the RF field.

Here ω_{pe} is the electron plasma frequency which is given by:-

$$\omega_{pe} = \sqrt{n_e e^2 / m_e \varepsilon_\circ} \tag{1.24}$$

And ω_{pi} is the ion frequency plasma and it is given by:-

$$\omega_{pi} = \sqrt{n_e e^2 / M_i \varepsilon_\circ} \tag{1.25}$$

Second is the high-frequency regime ($\omega_{pe} \ll \omega_{rf} \ll \omega_{pi}$). In this regime, the frequency of plasma ions is less than the radio frequency (ω_{rf}) and electron frequency (ω_{pe}). Due to the slow motion of ions, it is considered to be stationary. Most of the time the low-pressure non-LTE of discharge operates in the second frequency regime.

Plasma discharges generated by RF are divided into two major types. Inductively coupled plasma (ICP or H-discharge) and capacitive coupled plasma (CCP or E-discharge). This classification is related to how the RF (electromagnetic field) is coupled to the discharge space.

1.7.2 Capacitive Coupled Plasma (CCP)

Capacitive Coupled Plasma (CCP) operates as a non-LTE system at low pressure, often called E-discharge due to the electric field initiating the discharge [36]. Within the chamber, reactive gases are present, and capacitive connected plasma forms between two electrodes, creating what is known as capacitive-linked plasma. This plasma involves two electrodes, one grounded and the other connected to the matching unit network as shown in Fig.1.4. Inside the plasma chamber, electrodes are placed in parallel. As ions move toward the cathode, the polarity of the electric field changes. This motion of ions between the electrodes occurs without sputtering or collisions.

The difference in potential between the powered electrode and the plasma is known as the bias voltage. When a substrate is placed on powered electrodes and undergoes bias voltage, the process is termed reactive ion etching. Reactive ions from the plasma, along with other species, contribute to etching the substrate. Within the plasma, two main parts exist: bulk and sheath. Bulk refers to the free quasi-neutral component of the central field, while sheath describes the non-neutral potential region near the surface [37]. The electric field within the sheath starts with positive charges and ends on the wall due to the negative potential. Thus, the surface becomes negatively charged regarding plasma.

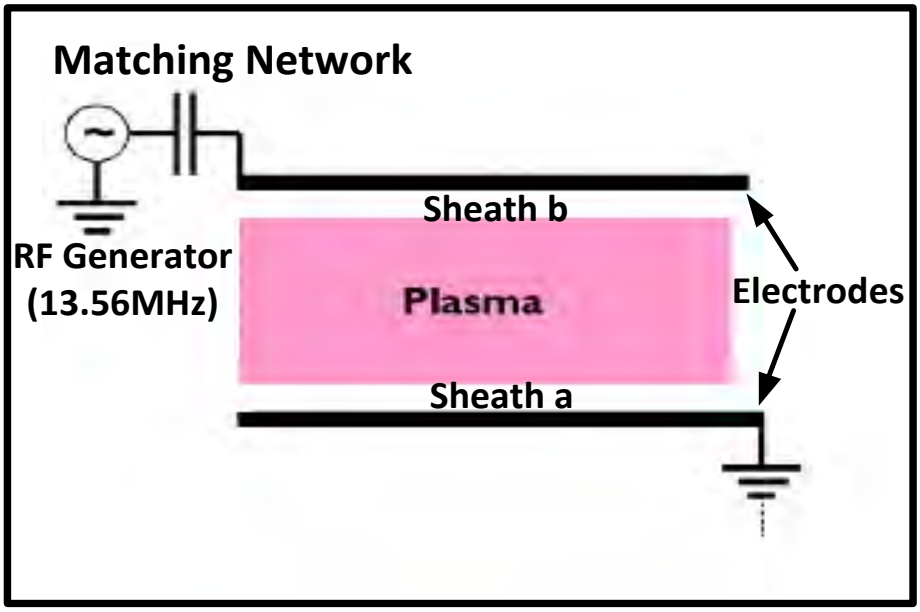

Figure 1. 4: Sketch of CCP arrangement.

Figure 1.5 shows the quasi-neutral bulk and the two-sheath formed adjacent to the electrodes in the CCP arrangement. Whenever there is a separation between electrons and ions, it will oscillate with a frequency of ω_{pe} and ω_{pi} correspondingly, where $\omega_{pi} = (e^2 n_i/\epsilon_0 m_i)^{1/2}$, is the "plasma-ion frequency" and $\omega_{pe} = (e^2 n_e/\epsilon_0 m_e)^{1/2}$ is the "plasma-electron frequency" [37].

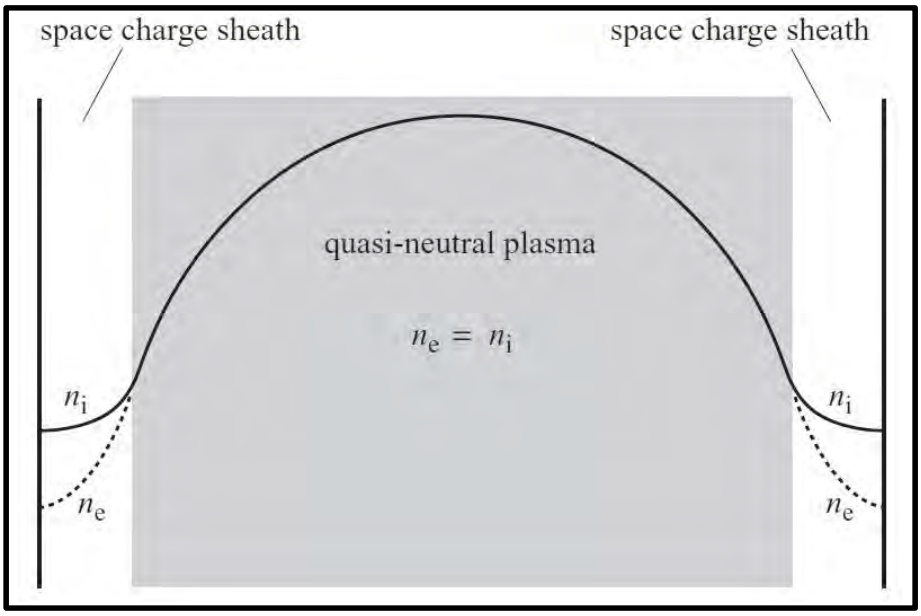

Figure 1. 5: Plasma bulk and time averaged position of sheath in a symmetric CCP [38].

Over time, the charged particle density varies in the sheath layer when the voltage is given to the electrode that has a frequency ω_{RF}. When $\omega_{RF} \gg \omega_{pi}$ then the ions cannot respond to the rapid fluctuating in potential and therefore only follow the time-averaged electric field in the sheath

Both sheaths are like the symmetrical configuration of the CCP system because the two electrodes have identical dimensions. The sheath will be dissimilar in width if the electrode within the discharge has a different area. When the plasma is present, the sheath forms around the grounded electrode and near the metallic vacuum container. An additional voltage drop occurred at the power electrode and this effect is known as the self-biasing [38].

When gas pressure is high then the energy is transmitted with the help of a collision heating process. In the heating process, the energy is combined by electrons during accelerated motion due to the electric field being transferred through collisions with other particles. In RF discharges the axial length of the quasi-neutral balk is greater than the time-averaged width of the sheath. While in the low-pressure region, the time-averaged width of the sheath is proportional to the axial length of the quasi-neutral bulk due to low plasma density and high voltage.

1.7.3 Inductively Coupled Plasma

An inductively coupled plasma (ICP) derives its energy from electric currents produced through electromagnetic induction using time-varying magnetic fields. One useful application of ICPs is detecting trace elements in environmental samples. The main function of ICPs is to emit specific wavelengths of light, which can be measured accurately. The technology behind the ICP system was initially used in the early 1960s to refine crystal-clear growth methods. Since then, ICP has been gradually employed and integrated with other processes for qualitative analysis.

The generation of plasma is very simple and low-cost with the help of CCP but there are some limitations associated with material processing applications. And the main disadvantage of CCP is that when the voltage is applied it causes the size of the sheath to decrease and changes the density of the plasma. For example, when we increase the applied power pressure it also increases and then the impurities within the chamber also increase which changes the chemistry of discharges.

At high pressure, a negatively charged particle that has a few micron sizes is produced and suspended above the target surface due to an electric field which can fall and damage the surface of the treated samples when the discharge is turned off. These problems are solved with the help of ICPs by using an external inductor coil which is known as an antenna in different configurations and that works on the principle of Faraday's laws of electromagnetic induction. There the time-varying magnetic induction $\vec{B}(t)$ induces the changing (time-varying) electric field $\vec{E}(t)$ given by:-

$$\nabla \times \vec{E}(r,t) = -\frac{\partial \vec{B}(r,t)}{\partial t} \tag{1.26}$$

Here in the above equation, $\vec{B}(t)$ is the magnetic field that is generated by the RF current flowing in the inductor coil that is separated from the discharge with the help of a dielectric window. Generally, for the generation of plasma in the laboratory, the cylindrical and planner coil configuration of ICPs is used. The cylindrical and planner coil configurations are shown in figure 1.6 and figure 1.7.

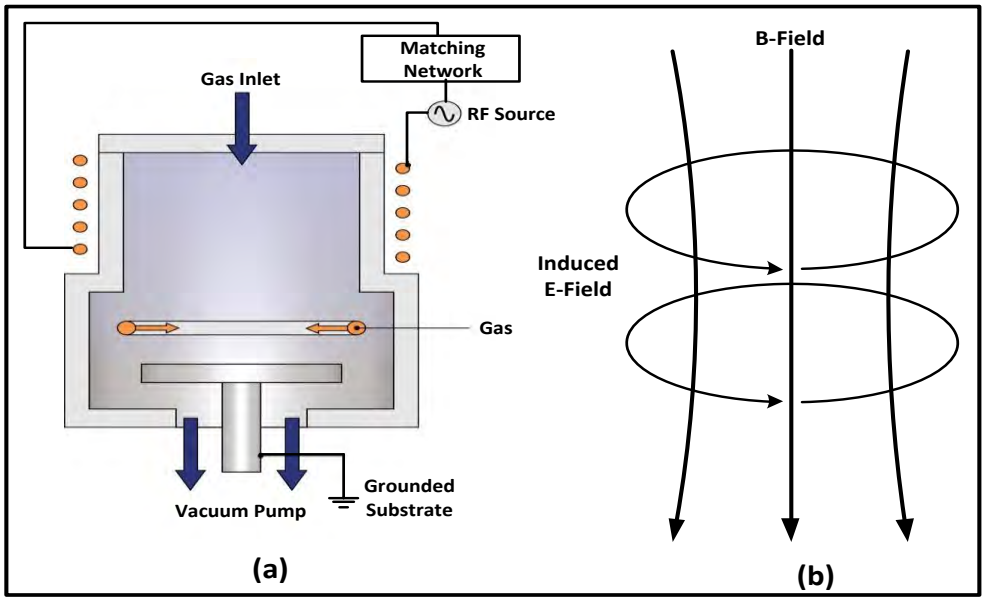

Figure 1. 6**:** (a) Sketch of Cylindrical ICP configuration (b) Direction of Magnetic and Induced Electric field.

In the cylindrical ICP setup, the RF coil surrounds the cylindrical chamber, while in the second configuration, a coil similar to a stovetop heating element (like a pancake) is positioned above the plasma chamber. In both types of ICPs, the electromagnetic field from the coil interacts with the plasma through a quartz glass (dielectric window), which separates the antenna (conduction coil) from the plasma. Low-pressure ICP discharges are characterized by low electron temperatures(T_e), high electron number densities(n_e) ($\sim 10^{10} - 10^{12} cm^{-3}$) and very thin, low-voltage sheaths compared to CCP.

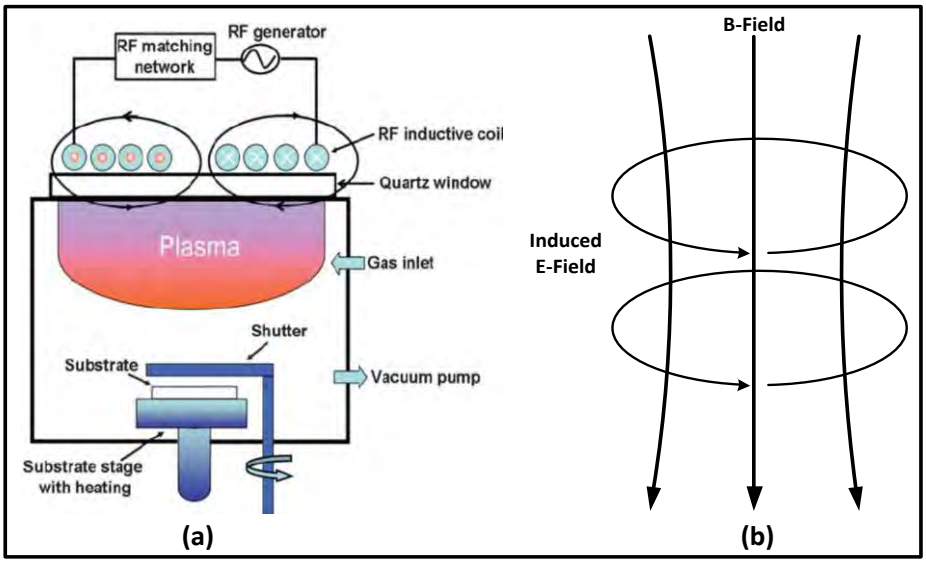

Figure 1. 7**:** (a) Sketch of Planner ICP Configuration (b) Direction of Magnetic and Induced Electric field.

In the arrangement of ICPs, RF sources are linked to the antenna coil through a matching unit, similar to CCPs. To achieve maximum efficiency with the matching unit, the RF coil electrically resonates for an RF output impedance of 50 Ω and at the driving frequency (13.56 MHz). Due to the matching effect, a significant amount of current flows in the conduction coil. Because of the higher time rate of change and current magnitude, a magnetic flux is generated in the adjacent region of the plasma (within the skin depth). This effect becomes more crucial at higher applied power. This effect has become more important with increasing applied power.

A high voltage across the coil ends is another result when the system is in resonance. These RF voltages are connected in the same manner as in the CCP and become more important at comparatively low applied powers. The terms capacity mode (E-mode) and inductive mode (H-mode) are commonly used to describe these regimes. MacKinnon was the first scientist who reported this [39]. ICP operates in one of two different ways that are based on the complete power controlled. The E-mode and H-mode details are listed below.

E-mode

The capacitive or electrostatic mode is commonly called the dark mode frequently and it is similar to the CCP discharge in appearance. The low electron number density($\sim 10^{8} - 10^{10} cm^{-3}$), of this mode is its defining feature [39]. This E-mode has low plasma density and limited light is usually present. The electrostatic field is generated by a high-voltage antenna and the ground discharge chamber is the cause of plasma formation in this mode. As a result, it is commonly referred to as an ICP capacitive mode**.** The electrostatic field is caused by a large potential difference between the charged (powered) and neutral (grounded) ends of the antenna coil. Due to the visible sheaths that are related to low density and the plasma behaves extremely close to the very low density of CCP discharges. CCP discharges are corresponding in terms of basic heat mechanisms **[**40].

In this state, both electron temperature and plasma potential are often high, yet the intensity of light emission remains very low. We can minimize the E-field with the help of Faraday shield or splitting the antenna coil into parts separated by suitable tuning capacitors. The practical inductive plasma processing source can function differently, depending upon the presence of electrostatic and induced electric field factors [41].

H-mode

The density of electrons rises with increasing the RF power. The induced electric field takes priority over the electrostatic field and causes their plasma generation. This H-mode is also known as inductive mode due to the power coupling and due to its great intensity of light. This mode is also known as a bright mode. ICP discharges in this mode are characterized by a high electron density ($\geq \sim 10^{11} cm^{-3}$) a comparatively low electron temperature(T_e), a low plasma potential(v_p), and slight sheaths with low power [42].

Due to the high electron density(n_e), which prefers the cover out of the RF field and heating is contained to the layer of the skin, the electron means energy is lower in the H-mode as compared to the E-mode. The RF current flowing through the coil, which also creates a magnetic field, creates an electric field known as an azimuthal electric field. As a result, the discharge develops a current that is directed in a reverse way from the RF current. This is identical to a transformer action and the power couple to the plasma is governed both by the generating as well as induced current, therefore the ICP is also known as TCP(transformer coupled plasma). The plasma potential is lowered as compared to the CCP sources because the induced electric fields accelerate the electrons in closed orbits by heating them and preventing them from escaping through the wall surface. The discharge electrons in H-mode are heated by both Oh-mic and stochastic heating due to the presence of electrostatic and induced fields. [40**].**

In reality, neither of the mode completely pure and both heating processes are present at the same time. According to the power applied any of them will control another and this state is known as a particular mode. By installing of Faraday shield between both the antenna and the quartz plates the impact of capacitive coupling can be decreased when operating under purely inductive mode. The electrostatic field is related to the antenna coil along with the induced field in plasma [43].

The presence of H and E modes as well as the movement from E-mode to H mode provides ICP more attractive due to the different properties of these discharges and related to the Physics changes in plasma properties such as particle density, current, plasma potential, and plasma brightness can usually generate the E and H modes transition [44]**.**

1.8 Applications of plasma

Technological advancements greatly shape the industry's evolution. The progress of industrial nations relies on creating effective methods to directly tackle issues and adapting

evidence-based implementations that suit regional needs. This continuous stream of new technology is contributed to an increase in the efficiency of technological growth. Increased job options and economic expansions result in improved living conditions for its population. The rare non-equilibrium temperature conditions in LTP result in highly reactive chemistry in a generally cold environment. As a result, LTP is extremely important in a wide range of technological and scientific uses. Biomaterials, microelectronics, biomedicine, defense aircraft technology, automobile companies, telecommunications, and optical production to name a few. The main purpose is two improve the properties of a material without disturbing the bulk properties.

i. Plasma Etching

The plasma etching method was utilized for the change of chemical and physical characteristics. This process is commonly used to make electronic components for the technological environment. Moreover, this method is used for the treatment of thin skin. When materials and devices are utilized in hydrogen plasma aging and it has been observed that such etching proves the process has been able to remove a portion of the local oxides in certain areas.

ii. Plasma Ashing

Plasma ashing is generally used to separate the organic compound from the surface of organic compounds and it is the method by which the photoresist from such an etching device. Plasma ashing typically uses a combination of gases made of fluorine or oxygen. Inorganic materials are turned into by the plasma ashing process. The vacuum pump pushes away the secondary products which are often in the form of water vapors and volatile carbon oxides.

iii. **Plasma Electrolytic Oxidation**

The process of coating light materials and their composite materials with a surface treatment to improve the substance's characteristics is referred to as micro Arc oxidation (MAO) and plasma electrolytic oxidation (PEO). By using this method steel becomes up to four times harder. The method of sterilization also is known as the use of low-temperature plasma and it is useful for washing and sanitizing any material’s surface [45].

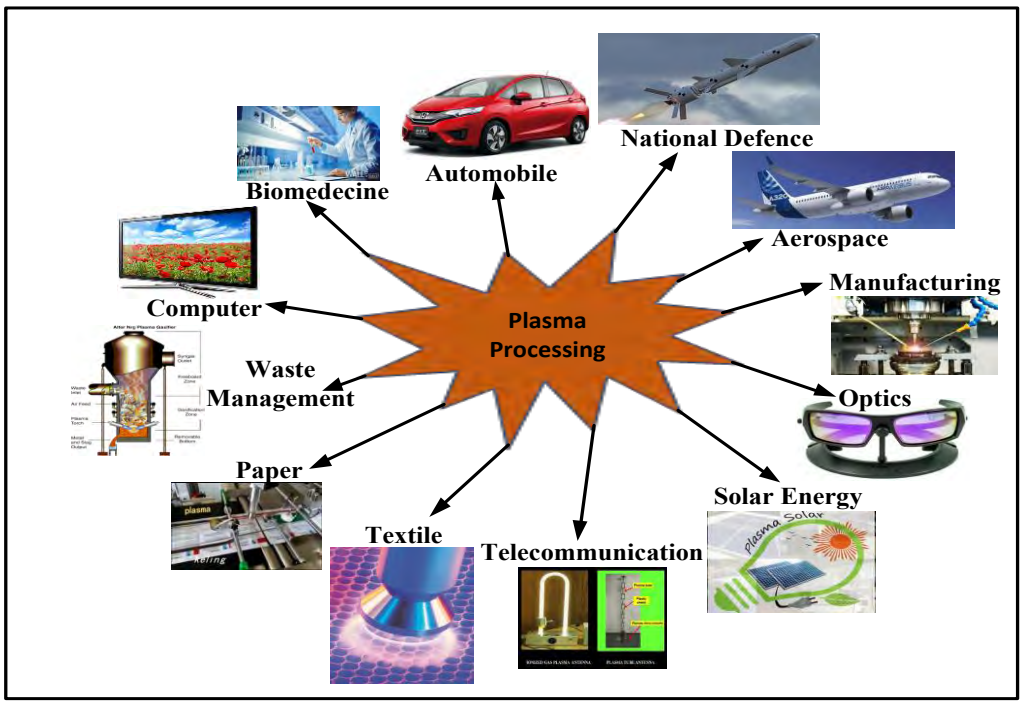

Figure 1. 8: Application of the Low Temperature Plasma in various industries.

iv. Plasma Vapor Deposition (PVD)

Utilizing plasma-enhanced chemical vapor deposition, a thin coating can be created on a material (PECVD). While during this process, plasma of the reactive gases is created following a chemical reaction with material particles. RF or DC devices are typically used to create such type of plasma and the reacting gases fill the space between the electrodes.

v. Cathode Ray Tube (CRT

Before digital technology television businesses employed cathode ray tube (CRT) displays which was a difficult technology. A breakthrough display technology known as a plasma display panel (PDP) and plasma-addressed liquid crystal (PALC) plasma have been developed over the past twenty years.

vi. Industrial Application of Plasma

It takes a sufficient amount of chemical energy and water to manufacture classical textiles. But the dry plasma process offers an alternate strategy for reducing the price of the essential materials. Plasma treatment is an important contribution to dry-cleaning in the textile industry. An accurate assessment is necessary to stop it from damaging the material. A basic study into the use of plasma in the manufacturing industry has been conducted in recent years [46].

Due to its ability to produce light, plasma finds numerous uses in the light industry such as fluorescent lamps. The first is for particles covered within the glass tube or further excited by the UV radiations released by plasma. The phosphorus particle subsequently emits visible radiation during the excitation mechanism. In both the home and the workplace, these lamps are widely utilized.

1.9 Layout of the Dissertation

In this dissertation chapter 1 includes detailed introduction to plasma and a discussion of the fundamental mechanism that is taking place inside the plasma. Various parameters, for example, plasma density, electron, and excitation temperature which characterize the behavior of plasma are also discussed here in detail. Various methods applied for the generation of plasma and sources of plasma, hot and cold plasma is discussed, plasma technologies and their applications are also given in chapter 1. Chapter 2 covers the brief introduction of “Langmuir Probe" plasma diagnostic tool. This chapter is divided into three sections. The first summarizes different diagnostic methods. The second section touches on the Child-Langmuir Law. Lastly, the third section delves into the Single Langmuir Probe's structure, function, and how it calculates plasma parameters like electron density and temperature from the probe's I-V characteristic curve. The chapter 3 explains various accessories used in the research work with a plasma-generating reactor. The setup includes the MaPE-ICP reactor, RF power generator, matching network, vacuum pumps, pressure gauges, and a motor pump for water circulation. The experimental setup is completed by a brief overview of plasma diagnostic methods, which involve using a single Langmuir probe (LP) with an RF compensated circuit. Chapter 4 describes the experimental results and discussion.

CHAPTER 02

PLASMA DIAGNOSTIC AND LANGMUIR PROBE

2.1 Plasma Diagnostics

Non-thermal plasmas are used a lot in different advanced production methods, especially in silicon integrated circuit (IC) technology where they have the biggest impact. The different reaction rates must be closely monitored to manage plasma processing correctly and the plasma parameters must be experimentally adjusted for the best outcomes. For this, a variety of non-intrusive and intrusive methods are employed, involving multiple probes and spectroscopy methods. The main focus of plasma diagnostics is the identification, classification, and characterization of the primary species involved in plasma processing. This includes learning about their energies, concentrations, and rate factors of the relevant reactions, among other things. Determining the main areas in charge of the plasma behavior is possible through a diagnostic process [47].

The most popular electrical diagnostic tool is the Langmuir probe which offers a straight forward and relatively inexpensive method for measuring plasma properties like electron density (n_e), electron temperature(T_e), and electron energy distribution functions (EEDF) in low-pressure plasmas [48, 49]. The features of the I-V probe contribute to calculating the plasma potential, temperature, and electron density. Emission spectroscopy can be used to identify plasmas that emit light [50, 51]. It's really common to identify excited species, calculate their number density, and determine their temperatures using this non-intrusive method.

The focus of the current study is on examining how plasma parameters effects with probe length variation. This relates to measuring active species electron density, electron temperature, plasma potential and electron energy distribution function. As plasma diagnostics Langmuir probe and optical emission spectroscopy are used.

2.2 The Child-Langmuir Law

This law explains the highest current density between two flat plates in a vacuum, set at a fixed voltage difference "φ" and placed at a distance from each other [52]. This law is also named the “three halves power law”.

To find the "Child-Langmuir law," we begin with Poisson's relation.

$$\nabla^2\varphi = -\frac{\rho}{\varepsilon_0} \tag{2.1}$$

In this equation, "ρ" stands for charge density. We assume the plasma sheath is mostly made up of electrons, so the charge density in the sheath is negative. In one dimension, the Poisson's equation can be written as:

$$\frac{d^2\varphi}{dx^2} = -\frac{\rho}{\varepsilon_0} \tag{2.2}$$

Put $J = nev = \rho v$, using this in Eq. 2.2:

$$\frac{d^2\varphi}{dx^2} = \frac{J}{v\varepsilon_0} \tag{2.3}$$

In the plasma sheath, if "φ" is the potential, electrons reach a velocity "v" within that area. We can write:

$e\varphi = \frac{1}{2}\, mv^2$ or $v = \sqrt{(2e\varphi/m)}$.

Therefore:

$$\frac{d^2\varphi}{dx^2} = \frac{J}{\varepsilon_0}\sqrt{\frac{m}{2e\varphi}} \tag{2.4}$$

Multiplying by $\frac{d\varphi}{dx}$ and integrating from sheath edge "x_S" to wall "x_W" bounded the plasma.

$$\int_{x_s}^{x_w}\left(\frac{d\varphi}{dx}\frac{d^2\varphi}{dx^2}\right)dx = \frac{J}{\varepsilon_0}\int_{x_s}^{x_w}\sqrt{\frac{m}{2e\varphi}}\frac{d\varphi}{dx}dx \tag{2.5}$$

$\Longrightarrow$

$$\int_{x_s}^{x_w}\left(\frac{d\varphi}{dx}\frac{d^2\varphi}{dx^2}\right)dx = \frac{J}{\varepsilon_0}\int_{x_s}^{x_w}\sqrt{\frac{m}{2e}}\varphi^{-1/2}\frac{d\varphi}{dx}dx \tag{2.6}$$

Put solution from Eq. ($\int_{x_r}^{x_w}\left(\frac{d\varphi}{dx}\frac{d^2\varphi}{dx^2}\right)dx\,\frac{1}{2}\left(\frac{d\varphi_w}{dx}\right)^2$) in LHS of above equation and solve RHS, we get:

$$\frac{1}{2}\left(\frac{d\varphi_w}{dx}\right)^2 = \frac{2J}{\varepsilon_0}\sqrt{\frac{m}{2e}}{\varphi_w}^{1/2}$$

$\Longrightarrow$

$$\frac{d\varphi_w}{dx} = \left(\frac{4J}{\varepsilon_0}\sqrt{\frac{m}{2e}}\right)^{1/2} (\varphi_w)^{1/4} \tag{2.7}$$

Re-arranging terms in above Eq. 2.7, we have:

$$\varphi_w{}^{-1/4}\, d\varphi_w = \left(\frac{4J}{\varepsilon_0}\sqrt{\frac{m}{2e}}\right)^{1/2} dx \tag{2.8}$$

Integrating Eq. 2.8 from the limit of sheath edge "x_s" to the wall "x_w" and solve the equation:

$$\frac{4}{3}\varphi_w{}^{3/4} = \left(\frac{4J}{\varepsilon_0}\sqrt{\frac{m}{2e}}\right)^{1/2} (x_w - x_s) \tag{2.9}$$

From Fig. 2.1, it is evident that from reference point "x_w", in term of sheath thickness "d" the distance of wall can be written as $x_w = x_s + d$. Putting this in Eq. 2.9, we have:

$$\frac{4}{3}\varphi_w{}^{3/4} = \left(\frac{4J}{\varepsilon_0}\sqrt{\frac{m}{2e}}\right)^{1/2} d$$

$\Rightarrow$

$$\frac{16}{9}\varphi_w{}^{3/2} = \frac{4J}{\varepsilon_0}\sqrt{\frac{m}{2e}}\, d^2$$

$$J = \frac{4\varepsilon_0}{9}\sqrt{\frac{2e}{m}}\frac{\varphi_w{}^{3/2}}{d^2} \tag{2.10}$$

Putting the values of constant in Eq. 2.10, we get

$$J = 2.33 \times 10^{-6}\frac{\varphi_w{}^{3/2}}{d^2} \tag{2.11}$$

Above equation gives the well-known Child-Langmuir Law.

2.3 Langmuir probe

Electrostatic Langmuir probes are one of the well-known plasma diagnostic methods, and they are frequently utilized because of their dependability and simplicity [53, 54]. A wired connection submerged in plasma whose I-V characteristics are measured using a reference electrode is the most basic type of Langmuir probe. A relationship between such I-V characteristics and plasma parameters including electron density (n_e), electron temperature

(T_e), plasma potential (v_p), and electron energy distribution function (EEDF) can be established by analyzing these I-V characteristics using an appropriate theory. American (Nobel Laureate) Scientist Irving Langmuir and his helpers initially presented it in the 1920s [4].

While being affordable, simple to build, and use generally. It has to make some compromises with complex probing hypotheses that could result in inaccurate data analysis. The loss of privacy of these probes, which ultimately effects the local discharge conditions, is another drawback of their use. When we put a probe into the plasma, a layer forms around its tip. This layer makes it hard to get the right data about the plasma because it blocks out some things [55].

2.3.1 Probe construction

A Langmuir probe is a very thin metal wire that's covered everywhere except at the very tip, where it touches the plasma. The probe tip mostly has a diameter of less than 1 mm (0.2mm) and the length is 5mm to 10 mm which is used in this study. The tip material has an extreme melting point and commonly used materials include platinum, tungsten, titanium, and molybdenum. The tungsten wire used to make the probe tip for the current study has a diameter of 0.2 mm and a length of 5 mm to 10 mm.

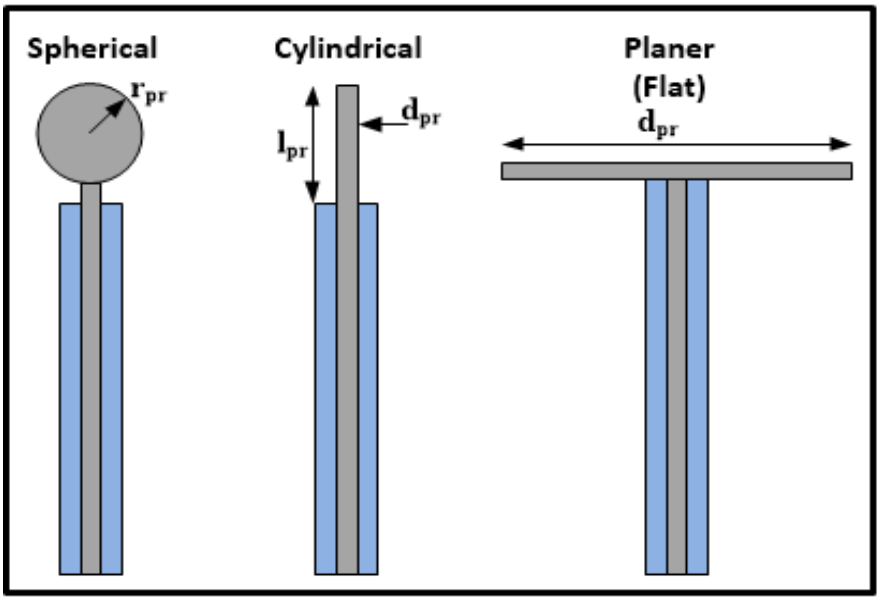

Figure 2. 1**:** Images of the probe tip spherical, cylinder and planar.

At present, the most commonly use of electrostatic-Langmuir probe is in semiconductor industry. The Langmuir probe has three configurations, which based on size and dimensions of probe tip.

i. Spherical probe

ii. Cylindrical probe

iii. Planer probe

As shown in figure 2.1.

In the present study, the single Langmuir probe with cylindrical tip has been used. The choice of the probe only depends on the characteristics of the plasmas which are of principle interest.

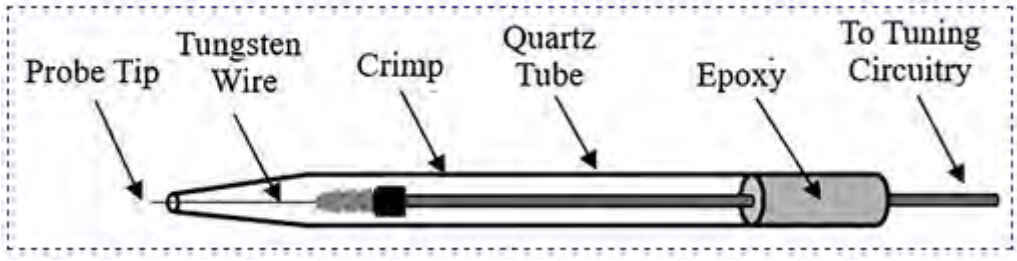

Figure 2. 2**:** The schematic diagram of a single Langmuir probe.

2.3.2 Working Principle of Langmuir Probe

The Single Langmuir probe is a wire that is used to measure the properties of plasma. The probe is connected to a reference electrode and has an electrical charge. As shown in figure 2.3 it is directly inserted into the plasma to measure the current from both electrons and positive ions.

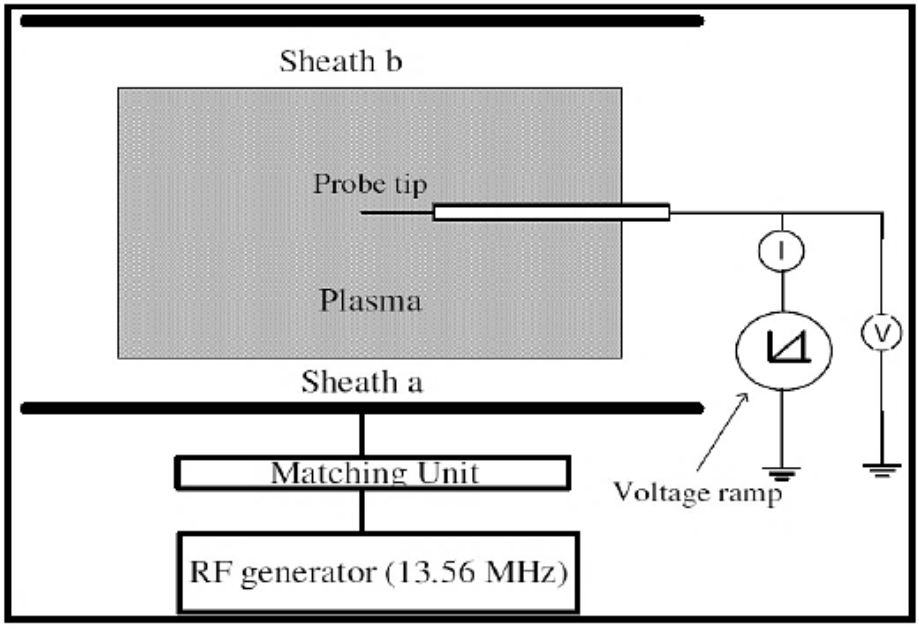

Figure 2. 3**:** The sketch of single LP measurement in CCP system [56].

To understand the behavior of the probe and the plasma, researchers create a graph called the IV characteristics. This graph shows the relationship between the current flowing through the probe and the voltage applied to it. By plotting the current against the voltage, researchers can analyze the behavior of the plasma and the probe. Druyvesteyn is a scientist who explained the IV characteristics of the Single Langmuir probe. His explanation helps to understand the electron velocity distribution function (EVDF) of the plasma. The EVDF describes the distribution of electron velocities within the plasma. The probe characteristics are analyzed using probe theory which makes the connection between the measured characteristics and the different parameters of undisturbed plasma. Probe theory gives an explanation to the understanding of the probe behavior.

2.4 I-V characteristics curve

When a probe tip is submerged in plasma, a sheath forms around it, bringing the bulk plasma to a point known as the plasma potential (V_p). Therefore, the potential that formed surrounding the probe surface can be mathematically expressed as $U = (V - V_p)$. Whenever the electron current equals the ion current, a floating stage has been reached, and the probe potential at this time is referred to as the floating potential (V_f). This acts as a barrier for the approaching electrons. This point is equivalent to the zero current point on an I-V curve.

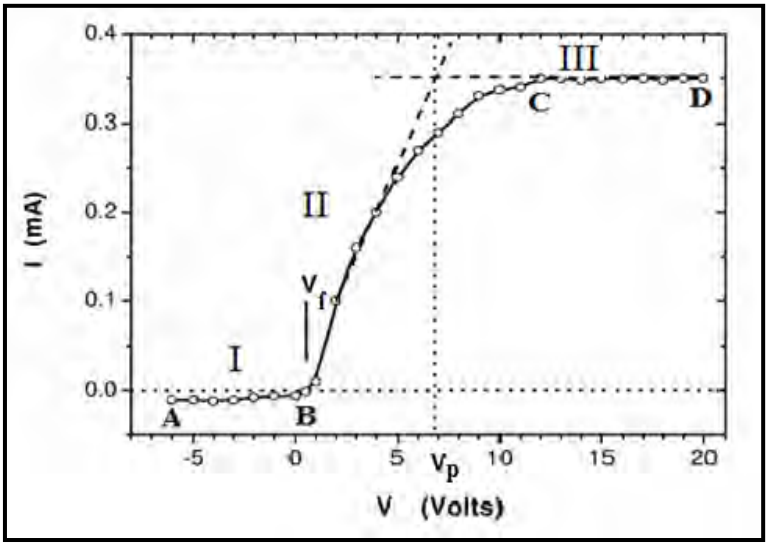

Figure 2. 4**:** A typical I-V characteristics curve measured from the LP [57].

According the Figure. 2.5, the I-V curve is separated into the following three sections to provide a thorough description of the probe properties.

2.4.1 Ion saturation current region $\left((\mathbf{V} \ll \mathbf{V_f}, \mathbf{V_p}) \textbf{ and } \mathbf{U} \ll \frac{\boldsymbol{KT_e}}{\boldsymbol{e}}\right)$

In this part, the probe gets only positive ions because it has a negative potential applied to it. This means that only positively charged particles, like ions, move toward the probe while the negatively charged particles, such as electrons, are repelled. If we increase the potential compared to V_f, there's a point where almost no electrons reach the probe. At that point, most of the current in the probe is made up of positive charges, like ions, rather than electrons. From ion saturation current (I_{is}), we can calculate the ion density (n_i). This current is controlled by the Bhom's velocity v_0 and can be written as [37].

$$\mathrm{I_{is}} = \mathrm{n_i e \langle v_o \rangle} \frac{\mathrm{A_p}}{4} \tag{2.12}$$

Here A_p is the area of the probe tip.

2.4.2 Transition or Electron Retardation Region ($\boldsymbol{V_f < V < V_p \textit{ and } U < \frac{KT_e}{e}}$)

When the negative potential is applied to the probe, reference to the V_f is reduced, and the electrons will overthrow the retarding force. At the small value of negative potential, the energetic electrons may reach the probe first. However, when V_p and the applied voltage on the probe get comparable, the low-energy electrons will also reach the probe surface. The negative ions of the electronegative plasma are also collected near the V_p because they have much lower energies compared to those of electrons [58].

The electron current (I_e), in this region of the I-V curve, changes exponentially with external potential. For a plasma obeying Maxwellian distribution, it can be written as follows [37]:

$$\mathrm{I_e} = \mathrm{I_o} * \exp\left[\frac{\mathrm{e(V - V_p)}}{\mathrm{kT_e}}\right] \tag{2.13}$$

By taking natural logarithm, it becomes:

$$\mathrm{lnI_e} - \mathrm{lnI_o} = \left(\frac{\mathrm{eV}}{\mathrm{kT_e}}\right) - \left(\frac{\mathrm{eV_p}}{\mathrm{kT_e}}\right) \tag{2.14}$$

Differentiate above equation with respect to voltage "V", we have;

$$\frac{\mathrm{d(lnI_e)}}{\mathrm{dV}} = \mathrm{e/k\,T_e} \tag{2.15}$$

From the graph between $ln\, I_e$ and V, we can obtain electron temperature (T_e) in the retardation region. The net current collected by the probe in this region is actually the sum of positive ion and electron currents. Consequently, the contribution of ion current requires to be corrected in order to determine electron temperature (T_e) perfectly.

2.4.3 Electron Saturation Region (V > V p and U> 0)

In region C of Fig. 2.2, the biasing voltage is higher than the plasma potential around it, shown by $v>vp$. The probe in this area collects the electron saturation current. At the probe tip, a negative sheath forms. Also, since electrons are lighter, their saturation current is often bigger than the ion saturation current [55]. If the probe gets a positive potential compared to V and we raise it slowly, the probe will collect the electron saturation current (I_{es}). This causes both negative ions and electrons to move toward the probe tip. The (I_{es}) in this region is described by:

$$\mathrm{I_{es}} = \mathrm{n_e e \langle v_e \rangle} \frac{\mathrm{A_p}}{4} \qquad (2.16)$$

2.5 The Probe Theory

The operation of the Langmuir probe for various I-V characteristics and collisions has been explained by a wide range of explanations. Whether the sheath is collisional or collision-less electron and ion flux. In low-pressure discharges, the electron means the free path is typically greater than the size of the probe tip and sheath. Electron dynamics in the sheath regions play an important role in determining that how many electrons can approach the probe tip. Secondly, in a collision-less collision, less mobility of the electron in the sheath regions is defined by the energy the electron has at the sheath boundary and the potential that appears across the sheath. The mobility of electrons in the sheath regions is described in this context by the most widely used theory that focuses on orbital motion restrictions. According to the Laframboise, Orbital Motion Limited (OML) theory is used to determine the electron (and ion) current [59, 60]. Therefore, just these few assumptions must be made in RF discharges to obtain almost accurate current relationships.

It is widely known that low-pressure RF plasmas have cold ions and few particle collisions, which leads to two essential hypotheses: a temperature difference between electrons and ions, (i.e. $T_e >> T_i$) as well as the absence of collisions in the plasma sheath.

Therefore, it is considered that the:

- The potential across the plasma sheath formed surrounding the probe is U=V−Vp, in which V is the applied probe voltage and Vp is the plasma potential.
- This potential fully develops across the sheath with no disruption to the plasma as a whole.
- At the sheath edge, the electron number density and their velocity distribution functions are well understood.
- Since they can pass through the sheath, all of the electrons are absorbed in the probe surface.
- To minimize plasma disturbance, the probe tip area is kept as tiny as possible.
- l which is considered to be the length of the probe tip is greater than the sheath width s ($l \gg s$) hence the velocity component along the cylinder surface that is along the z-axis does not to the current density i.e. $v_{ZS} = 0 = v_{ZP}$.

$$f(v_S) = f(v_{RS}, v_{TS}, v_{ZS})\, dv_{RS}, dv_{TS}, dv_{ZS} \tag{2.17}$$

The above formula is used to calculate the number of electrons per unit volume that arrive at the sheath edge "s" with a velocity of v_s that includes components of radial velocity between v_{RS} and $v_{RS} + dv_{RS}$, tangential velocity between v_{TS} and $v_{TS} + dv_{TS}$ and perpendicular velocity (parallel to the tip axis) between v_{ZS} and $v_{ZS} + dv_{ZS}$.

The current generated by the flow of incoming electrons passing through the sheath is given as:

$$dI_e = Aev_{RS}f(v_{RS}, v_{TS}, v_{ZS})\, dv_{RS}, dv_{TS}, dv_{ZS} \tag{2.18}$$

In the above equation, A is the area of the probe tip and A=$2\pi sl$. However, the orbital motion of the electrons in the sheath must be investigated to ascertain the electron flux reaching the probe surface as shown in Fig. 2.5. The sheath edge and probe surface show momentum and energy conservation, and the related velocity components are as follows:

$$v_{TS}s = v_{TP}R_p \tag{2.19}$$

So from the above equation, we can write:

$$\frac{1}{2}m_e(v_{RS}^2 + v_{TS}^2 + v_{ZS}^2) - eU = \frac{1}{2}m_e(v_{RP}^2 + v_{TP}^2 + v_{ZP}^2) \tag{2.20}$$

From above equations 2.18 and 2.19 putting the v_{TP} with noting that $v_{ZS} = 0 = v_{ZP}$, and $l \gg s$. Hence the velocity of v_{RP}^2 can be written as:

$$v_{RP}^2 = v_{RS}^2 - v_{TS}^2\left[\left(\frac{s}{R_p}\right)^2 - 1\right] + \frac{2eU}{m_e} \tag{2.21}$$

To get an electron to the probe tip, $v_{RP}^2 \geq 0$; v_{RP} is a "necessary" (but not sufficient) requirement v_{RP} should not evaporate between s and R_p.

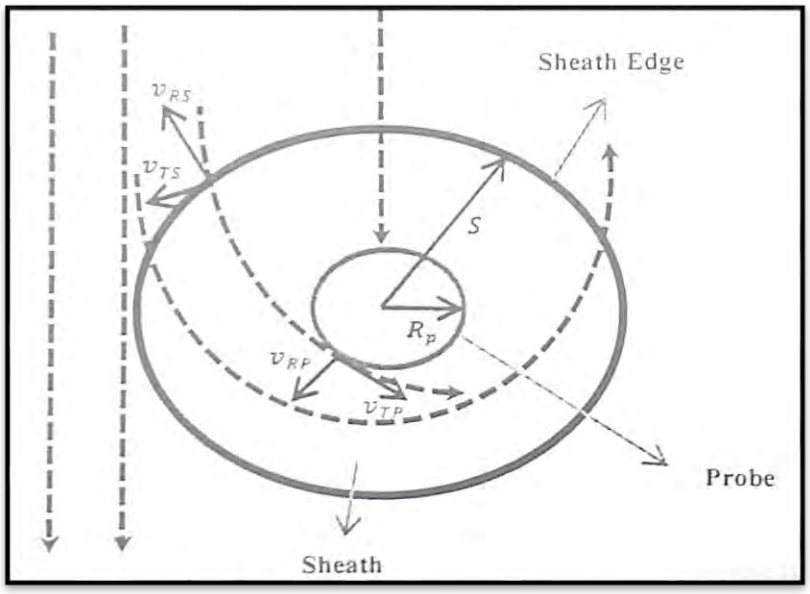

Figure 2. 5**:** Particle Trajectories around the probe tip in the presence of a sheath [60].

This means that the electron at the sheath boundary (s) should have a tangential velocity that is lying between them.

$$0 \leq v_{TS}^2 \leq \left(v_{RS}^2 + \frac{2eU}{m_e}\right)\left[\left(\frac{s}{R_p}\right)^2 - 1\right]^{-1} \tag{2.22}$$

2.5.1 The Electron Saturation Current

The greatest current a probe may draw from the discharge is called the electron saturation current, and it can be calculated by integrating Eq. 2.18 for all potential velocities as follows:

$$I_{es} = Ae\int_{v_{RS=0}}^{\infty}\int_{v_{TS}=-v_{TS}(max)}^{v_{TS}(max)}\int_{v_{ZS}=-\infty}^{\infty} v_{RS} f(v_{RS}, v_{TS}, v_{ZS})\, dv_{RS}, dv_{TS}, dv_{ZS} \tag{2.23}$$

By using equation 2.22:

$$v_{TS(max)} = \pm\left(v_{RS}^2 + \frac{2eU}{m_e}\right)\left[\left(\frac{s}{R_p}\right)^2 - 1\right]^{-1/2} \tag{2.24}$$

As we already know that at the sheath edge ions are cold and electrons contribute to the Maxwellian distribution [59]:

$$I_{es} = Aen_e\sqrt{\frac{KT_e}{2\pi m_e}}\left[\frac{s}{R_p}\{1 - \text{erf}(\alpha)\} + \exp\left(\frac{eU}{kT_e}\right)\text{erf}(\beta)\right] \quad (2.25)$$

In the above equation, $\alpha = \sqrt{\frac{eU}{KT_e\left(\frac{s}{R_p}\right)^2 - 1}}$ and $\beta = \sqrt{\frac{eU}{KT_e 1 - \left(\frac{R_p}{s}\right)^2}}$While the error function can be defined as $erf(\Delta) = \frac{2}{\sqrt{\pi}}\int_{\Delta}^{\infty}\exp(-x^2)dx$. Hence from the above equation, it's completely clear that the sheath thickness and the radius of the probe tip, in addition to the sheath potential, affect the electron saturation current. Let's suppose that $s \gg R_p$then the electron current becomes proportional to the $U^{1/2}$ as given below [33]:

$$I_{es} = 4Aen_e\sqrt{\frac{kT_e}{2\pi m_e}}\sqrt{1 + \frac{eU}{kT_e}} \quad (2.26)$$

2.5.2 Retardation current of the electron

The electrons will overcome the restricting force when the negative potential given to the probe, concerning the v_f is decreased. The probe may be first reached by the energetic electrons at low negative potential values. Therefore, low-energy electrons will also reach the probe area when the supply voltage V on the probe becomes equivalent. Due to their far lower energies than electrons, the electronegative plasma's negative ions are likewise gathered close to the V [22].

In this part of the I-V curve, the electron current (I_e) varies rapidly with external potential. For a plasma obeying the Maxwellian distribution is [60].

$$\left(\text{dln}I_e/\text{dV}\right) = e/kT_e \quad (2.27)$$

We can determine the electron temperature (T_e) in the region of a delay from the graph between lnl_e and V. The probe's total current in this area is the result of adding the currents of positive ions and electrons. As a result, to precisely measureT_e, the impact of the ion current must be adjusted.

The radial velocity required for an electron to go from the sheath to the probe tip at U < 0 is $v_{RS\,(min)} = \sqrt{-2eU/m_e}$ so the retardation current will become like given as follow:

$$I_{er} = Ae \int_{v_{RS}=v_{RS(min)}}^{\infty} \int_{v_{TS}=-v_{TS(max)}}^{v_{TS(max)}} \int_{v_{ZS}=-\infty}^{\infty} v_{RS} f(v_{RS}, v_{TS}, v_{ZS}) \, dv_{RS}, dv_{TS}, dv_{ZS} \quad (2.38)$$

For the Maxwellian electron density distribution at the edge, U becomes the exponential function. Hence I_{er} can be written as:

$$I_{er} = Aen_e \sqrt{\frac{kT_e}{2\pi m_e}} \exp\left(\frac{eU}{kT_e}\right) \quad (2.29)$$

2.5.3 The ion saturation current

As a result of the application of negative potential, the only current flowing to the probe in this location is made up of positive ions. When this potential is raised about V, practically no electrons will enter the probe at some voltage value, and the current flowing inside the probe is primarily caused by positive charges. The ion density (n_i) can be determined from the ion saturation current (I_{is}). With the help of Bhom's velocity (v_o), this current has controlled, which can be written as follows [37].

$$\mathbf{I_{is} = n_i e < v_o > \frac{(A_p)}{4}} \quad (2.30)$$

Here A_p denoted the area of the probe tip.

This is caused by electron diffusion, which creates a differential in density and an electric field in the pre-sheath that pulls the ions in that direction. Additionally, this gives the ions Bohm velocity so they can enter the sheath edge. As a result, the ion's thermal velocity (v_{iT}) and radial velocity (v_{iR}) are now significantly different. As a result, at the sheath edge, the ion's tangential velocity is zero [15]. As a result, the probe will attract the fast-moving ions entering the sheath.

As a result, every ion that enters the sheath is absorbed by the probe, making the sheath's width an efficient radius for capturing ions around the probe. It is discovered that the ion saturation current is:

$$I_{iS} = -JA_{Eff} \quad (2.31)$$

In the above equation, $A_{Eff} = 2\pi sl$ and s can be calculated by the C-L Law and J is known as the space charge current density so the ion saturation current becomes:

$$I_{iS} = -2\pi l \sqrt{\frac{4\varepsilon_0}{9}\left(\sqrt{2e/M_i}\right)V^{3/2}} \quad (2.32)$$

2.6 Plasma Parameter Calculations

A number of plasma properties, including electron density (n_i) and electron temperature (T_e), can be measured by using the probe I-V characteristics and their first and second derivatives. The collection of plasma parameters from the properties of the probe is briefly described below.

2.6.1 Floating (V_f) and plasma potential (V_p)

The floating potential V is the probe biasing voltage at which the ion saturation current (I_{is}) equals the electron repulsion current (I_{er}). The graphic representation of this location on the I-V characteristics is shown in figure 2.6. When the electron repulsion current (I_{er}) transforms into the electron saturation current les, the plasma potential V is the potential at that point. This point can be observed on an I-V characteristic curve, where the current passes through zero [33].

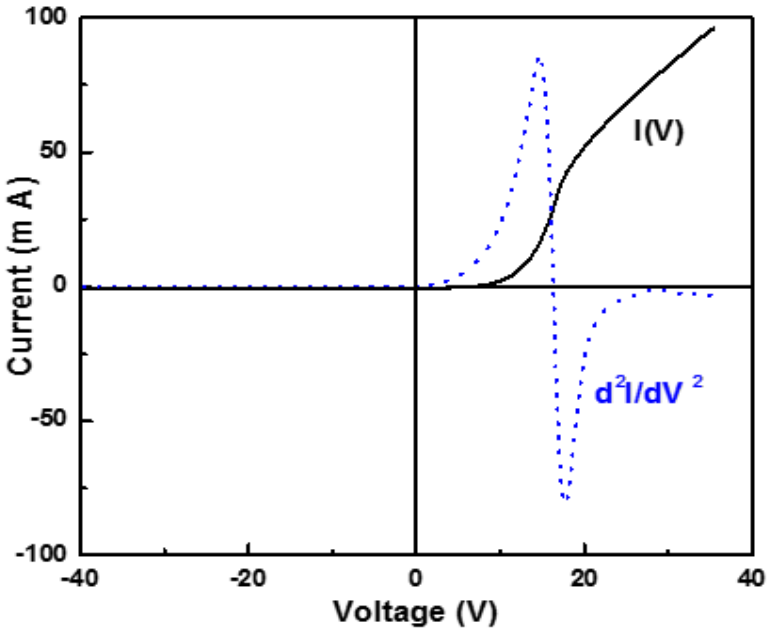

Figure 2. 6**:** Typical I-V characteristics curve and its second derivative of a single cylindrical probe [57].

$$V_f = V\ (I_{er} + I_{ir} = 0) \quad (2.33)$$

The V_p is the DC bias potential where the probe and plasma bulk are at the similar potential. The space potential (where $\mathrm{U} = \mathrm{V} - \mathrm{V_p} = 0$) correspond to a potential at the I-V curve where the transition of electron retarding current (feeling repelling potential) takes place into electron-saturation current (feeling attracting potential). The V_p can be easily obtained from the maximum of first derivate $I'(V_B)$ or from the point where the second derivative $I''(V_B)$ crosses zero (taken with respect to the applied potential to the probe surface).

2.6.2 Electron Temperature (T_e)

In a plasma, it's assumed that electrons are in thermal equilibrium. To calculate electron temperature (T_e) a Maxwellian distribution is considered [32]. The temperature term specifically represents the energy of a particular part of the distribution function in non-equilibrium discharges. In the context of a Maxwellian Electron Energy Distribution Function (EEDF), the slope of the lnI_{er} versus U plot helps determine the electron temperature.

$$\mathrm{lnI_e} = \frac{\mathrm{eU}}{\mathrm{kT_e}} + \frac{1}{2}\ln\frac{\mathrm{kT_e}}{2\mathrm{m_e}} + \mathrm{C} \tag{2.34}$$

While in the semi-plot graph, this equation gives the yield of a straight line and the slope will be related to T_e as:

$$\frac{\mathrm{kT_e}}{\mathrm{e}} = \left[\frac{\Delta\ln(\mathrm{I_{er}})}{\Delta\mathrm{U}}\right]^{-1} \tag{2.35}$$

If the plot deviates from being linear, it indicates a departure from the Maxwellian Electron Energy Distribution Function (EEDF). In such cases, the derived electron temperature (T_e) is more of an approximate estimate than a precise one. An alternative method to calculate electron temperature involves using the second derivative of the probe current for a Maxwellian distribution.

$$\frac{\mathrm{kT_e}}{\mathrm{e}} = \left[\frac{\Delta\ln(\ddot{\mathrm{I}}_{\mathrm{er}})}{\Delta\mathrm{U}}\right]^{-1} \tag{2.36}$$

However, for discharges with non-Maxwellian distributions, such as bi-Maxwellian distributions, either it is common to determine the average electron energy instead of temperature, or even the temperature of the various regions of the EEDF is determined independently. The effective electron temperature ($\mathrm{T_{eff}}$) is determined by the average energy like that$< \mathrm{E} >= \frac{3}{2}\mathrm{kT_{eff}}$.

2.6.3 Electron Energy Probability Function (EEPF)

In this range, only energetic electrons reach the probe, and the retarding current area in the I-V characteristics reflects information about their energy distribution. Langmuir initially proposed determining the Electron Energy Distribution Function (EEDF) by taking the second derivative of the probe current with respect to biasing voltage [11]. Druyvesteyn later confirmed that this method is effective for figuring out the EEDF, applicable to both cylindrical and planar probes.

When the electron mean free path is much larger than the sheath width and probe radius (e >> s, Rp), creating a collision less sheath, the total electron energy remains unaffected. In this scenario, even with fluctuations in the electric field near the probe, the electron velocity distribution does not change significantly. Consequently, the electron current in the electron retardation area, where a potential U=V-Vp exists across the plasma sheath, takes a specific form.

$$I_e = \pi eA \int_{-\infty}^{\infty} dv_x \int_{-\infty}^{\infty} dv_y \int_{v_{min}}^{\infty} dv_z v_z f_e(v) \quad (2.37)$$

In the above equation here $v_{(min)} = \sqrt{\frac{2e(V_p - V)}{m}}$ is the minimum velocity of an electron at the sheath edge to reach the probe surface. For an isotropic electron distribution, physical quantities solely depend on electron velocity. In such cases, the electron current follows a specific form.

$$I_e = eA \int_{-\infty}^{\infty} dv_x \int_0^{\theta_{min}} d\theta \int_0^{2\pi} d\varphi \, v\cos\theta v^2 \sin\theta f_e \quad (2.38)$$

Here $cos^{-1}\left(\frac{v_{min}}{v}\right) = \theta_{min}$ after the integrations of $\theta \; and \; \varphi$ the current will become:

$$I_e = \pi eA \int_{v_{min}}^{\infty} dv v^3 \left(1 - \frac{v_{min}^2}{v}\right) f_e(v) \quad (2.39)$$

The transformation in the above equation, 2.39 allows for the determination of f_e in terms of the second derivate of I_e concerning the U=V-V_p. With changing the variable <E>=$\frac{\frac{1}{2}mv^2}{e}$ that leads to:

$$I_e = \frac{2\pi e^3 A}{m^2} \int_V^{\infty} dE \, E\{(1 - V/E) f_e[v(E)]\} \quad (2.40)$$

Here $v(E) = \sqrt{\frac{2eE}{m}}$ differentiating we get:

$$\frac{dI_e}{dV} = -\frac{2\pi e^3 A}{m^2}\int_V^{\infty} dE\ f_e\,[v(E)] \tag{2.41}$$

$$\frac{d^2 I_e}{dV^2} = \frac{2\pi e^3 A}{m^2}\, f_e[v(E)] \tag{2.42}$$

Therefore the electron energy distribution function (EEDF), $g_e(E)$ is given as:

$$g_e(E)dE = 4\pi v^2 f_e(v)dv \tag{2.43}$$

Using the relation between E and v we will obtain:

$$g_e(E) = 2\pi\left(\frac{2e}{m}\right)^{3/2}\sqrt{E} f_e[v(E)] \tag{2.44}$$

Eliminating f_e from the above equation 2.29:

$$g_e(E) = \frac{2m}{e^2 A}\sqrt{\frac{2E}{m}}\,\frac{d^2 I_e}{dV^2} \tag{2.45}$$

The electron energy probability function (EEPF) is sometimes introduced as:

$$g_p(E) = \frac{g_e(E)}{\sqrt{E}} \tag{2.46}$$

It appears that the only variation between EEDF [eV^{-1}] and EEPF [$eV^{-3/2}$] is in the units; the shape is what distinguishes them [16]. Due to the lack of $\sqrt{eU}$ term, EEPFS has developed into a useful tool for differentiating between different distribution functions. Since the EEPFS in this situation may be immediately connected to the probe current's second derivative, it is simple to discriminate between the various potential distribution functions.

Once the EEDF has been determined, it is simple to estimate plasma properties including electron density (n_e), electron temperature (T_e), and plasma potential (v_p),). By integrating the EEDF, the electron density can be calculated as follows:

$$n_e = \int_0^{E_{max}} g(E)dE \tag{2.47}$$

The average energy can also be determined by dividing the total electron energy by electron density:

$$< E > = \frac{\int_0^{E_{max}} Eg(E)dE}{\int_0^{E_{max}} g(E)dE} \tag{2.48}$$

2.6.4 Electron Density

Once the plasma potential and electron temperature are determined, the electron retardation current (I_{er}) can be utilized to calculate the electron density in a discharge.
At V=V_p & U=0 so we can write electron density will be as follows:

$$n_e = \frac{1}{Ae}\sqrt{2\pi m_e / kT_e}\, I_{er} \tag{2.49}$$

The accuracy of measurements using this technique relies solely on precise plasma potential measurements. Because of the exponential nature of I_{er}, even a small error in estimating V can result in incorrect calculations of electron density (n_e). Another method involves squaring the electron saturation current (I_{es}) to determine electron density (n_e).

$$I_{er}^2 = 16\pi A^2 e^2 n_e^2 \frac{kT_e}{2\pi m_e}\left(1 + \frac{eU}{kT_e}\right) \tag{2.50}$$

This becomes the equation of the straight line and here the slope of I_{er}^2 concerning U which to the proportional of n_e^2 and hence given the electron density as:

$$n_e = \sqrt{\frac{m_e}{8A^2e^3}\frac{\Delta I_{es}^2}{\Delta U}} \tag{2.51}$$

2.7 Probe Cleaning

Probe cleaning methods are crucial in maintaining the accuracy and reliability of analytical instruments, particularly those used in Inductively Coupled Plasma (ICP) systems. In ICP, the sample introduction system includes a probe consisting of a nebulizer, spray chamber, and torch. Keeping these components clean is essential to prevent cross-contamination between samples and ensure the longevity of the equipment. Some ICP instruments come equipped with automated functions, including probe cleaning cycles. These automated cycles can be programmed to run at specific intervals or as needed, providing a convenient and efficient way to maintain the instrument's performance. Heat cleaning is another method where the probe is subjected to elevated temperatures to burn off organic residues. This is especially effective for removing organic contaminants that may accumulate during sample introduction.
The Langmuir probe is strong and easy to use, but a common problem is contamination. To clean it, heat the probe with electron bombardment, using a refractory metal for the tip. To do this, apply a bias of around +100 V and draw about 60 mA of current, usually in argon.

This is done with just a few watts of applied energy and pressures between 76 mTorr and 152 mTorr (0.1–0.2 bar). To endure ion bombardment, the probe needs to stay clean, achieved by applying a negative potential to it.

Gases like Ar or H_2 can be cleaned using this method. A stricter protocol must be used for more complicated plasma systems, such as those used for etching processes. Excessively high electron temperature, hysteresis in the I-V characteristic, and drift in the values of plasma parameters are all signs of probe contamination. If the probe is biased near plasma potential for more than a few seconds, it becomes polluted. It is advised that the probe be examined for a brief amount of time because of this. The smart soft system is equipped with both manual and automatic cleaning features for the probe tip. In the probe cleaning process, the pulse biasing voltage is adjusted from 10 to 100 V, and the power delivered to the probe tip is measured. The smart soft system maintains the power at a predetermined set point by adjusting the duty cycle. Additionally, the system automatically compensates for variations in external conditions, such as changes in power and pressure.

However, this self-compensation function may not be effective in the following condition.

- Very thick deposit layer.
- When applied voltage is comparable or several volts higher than plasma potential in density of plasma $\sim 10^{12}\ cm^{-3}$.
- In low density plasma ($\sim 5 \times 10^{7} \rightarrow 5 \times 10^{8}\ cm^{-3}$).

CHAPTER 03

INSTRUMENTATION AND EXPERIMENTAL SETUP

3.1 Plasma Generation System

The image of the diagnostic equipment and experimental setup utilized for plasma formation is shown in Figure 3.1. T. Meziani et al. provided the first description of MaPE-ICP.

Figure 3. 1**:** A picture of the experimental setup that was used in this study [61].

In Figure 3.2 the reactor is designed cylindrically with a planar coil embedded in a ferrite core material positioned above it. The MaPE-ICP system modifies the proprietary ferrite core material, increasing the magnetic field concentration by four times compared to a traditional ICP system. Using a solid, hard magnetic core material is crucial, acting as a vacuum seal and facilitating easier system scaling. In this case, the dielectric window's mechanical function is diminished, serving as an insulating wall between the coil and the plasma. Reducing its thickness increases the mutual inductance between the coil and the plasma.

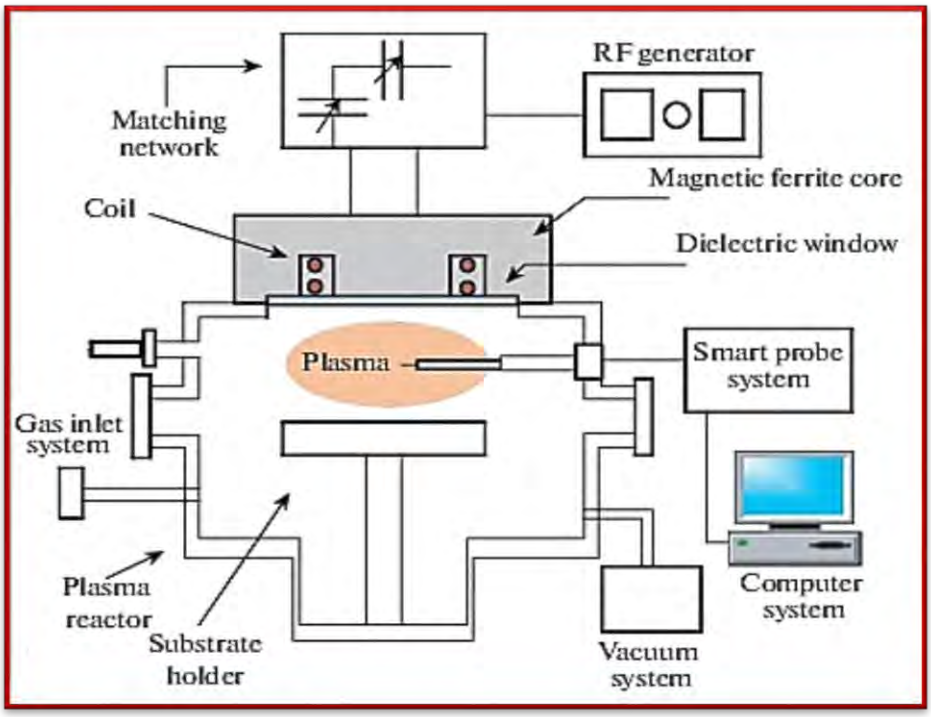

Figure 3. 2**:** An image of the MaPE-ICP source and diagnostics tool.

3.1.1 Plasma Reactor

The discharge chamber, locally manufactured, is cylindrical and made of stainless steel. It has an inner diameter of 34 cm and a height of 25 cm. There are many ports available for the injection of gases, probe insertion, and pressure gauge connection. A viewing window made of quartz glass is also provided to watch the discharge and record the spectrum using a spectrometer from inside the chamber.

3.1.2 Radio Frequency Generator

A power source of model PGF-RF Generator-1600 watt (its power ranges from 0 to 1600 watt with a 1watt step) was used via a matching network unit for plasma generation in the MaPE-ICP reactor (PFM-3000 A). The RF generator has fixed frequency is 13.56 MHz and characteristic impedance is 50.

The applied power in the MaPE-ICP system was calculated by comparing forwards and reflected powers. An essential aspect of MaPE-ICP is addressing the difference in impedance between the plasma and the RF generator. The typical mismatch can lead to inefficient power delivery to the plasma and result in harmful input power reflection, potentially damaging the RF supply. To mitigate this, an L-type impedance matching network with two units, a control unit and a tuning unit, was employed in the current study.

The tuning unit consists of variable capacitors and inductors as matching components. This matchbox configuration automatically adapts to minimize reflected power, ensuring efficient power delivery to the plasma and protecting the RF supply.

3.1.3 Matching Network Unit

Another important part of this setup is the matching network unit. Because the plasma and RF generator have a substantial impedance difference, external power cannot efficiently reach the plasma and is reflected back to the power source. The primary function of the matching network is to adjust the impedance of the plasma and RF generator, ensuring the maximum amount of power is delivered to the plasma and minimizing the reflection of input power.

In the current research project, an L-type impedance matching network with control and tuning units is utilized. The tuning unit comprises a combination of variable capacitors and inductors. The matchbox has various operating modes, but for the current experiment, it is set to automatic mode. In this mode, the matching network self-adjusts to achieve an optimal value, ensuring minimal RF power reflection.

3.1.4 Cooling system

To prevent overheating of the chamber, RF generator, matching network, and vacuum pump, a chilled water setup is implemented. This setup utilizes pure, decalcified water to cool these components. A motor pump is employed to circulate the cooled water throughout the entire system, effectively maintaining the temperature within the desired range.

3.1.5 Monitoring System and Pressure Controlling

With the aid of a turbo molecular pump and rotary pump, the reactor pressure was reduced to a base pressure of around 10^{-3}Pa. The Pirani and Penning gauges were used to measure the reactor's internal pressure. Hasting mass flow meters were used to gauge the flow rate of the working gases.

3.2 Plasma Diagnostics

Plasma diagnostics involve using different techniques, tools, and experimental approaches to measure various characteristics of the plasma. In the current study, RF compensated Langmuir probe (LP) technique is employed to calculate and estimate the various plasma parameters.

3.2.1 Langmuir Probe

The structure of the RF compensated probe used in this study is shown in Figure 3.3 and it is manufactured by Smart Probe Scientific System Limited. The probe tip is constructed to form 10 mm long tungsten wire with a radius of 0.1 mm. To collect data for calculating plasma parameters, the probe tip was inserted into the discharge at an axial position (between the quartz window and lower substrate holder) and radially midway. This insertion method allowed for accurate measurement and analysis of plasma characteristics.

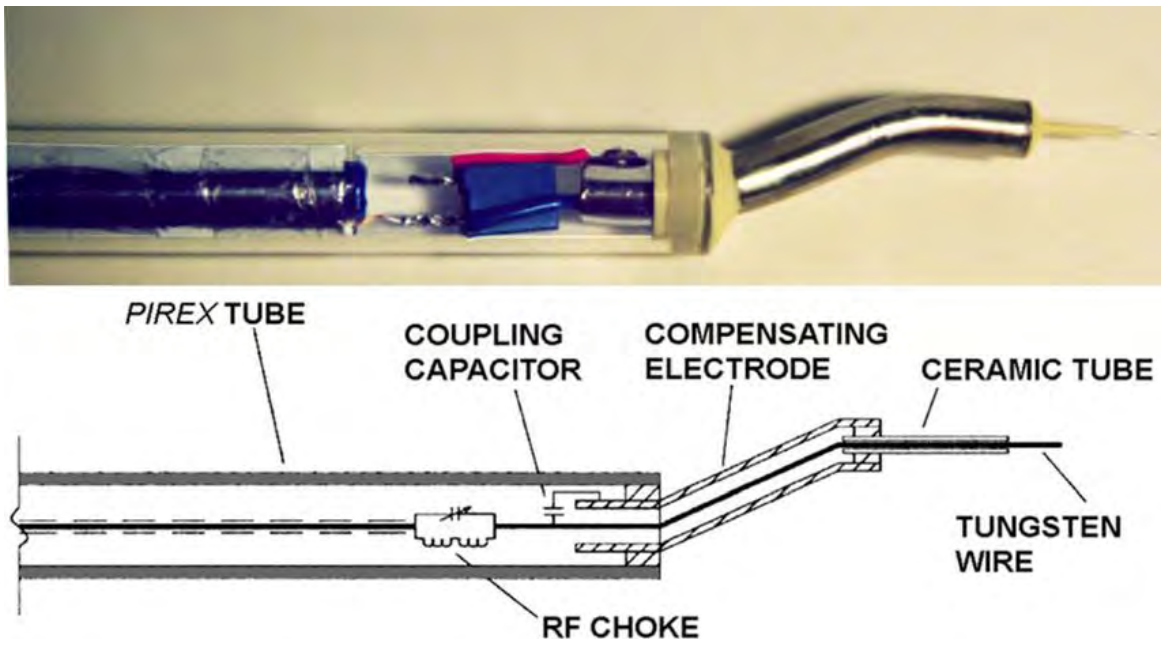

Figure 3. 3**:** Structural diagram of the LP [61].

3.3 RF compensation

In the past, significant efforts have been made to address RF distortions in Langmuir probe readings [62]. To accurately extract information from the recorded I-V characteristic curve while blocking RF interference, filtering becomes essential. RF distortions not only lead to inaccuracies in interpreting the space potential but also affect the low-energy portion of the Electron Energy Distribution Function (EEDF). In the H-mode of an inductively connected discharge, where plasma sheaths resemble a DC discharge, RF distortions are not a major concern. However, during transitions from the E- to H-mode, especially with a prominent E component, RF distortions have been observed [63].

In contrast to regular probes, the Smart Probe used in this study incorporates an additional compensating electrode and multiple inductors. A capacitor connects this electrode to the Langmuir probe tip, ensuring that the voltage on the electrode closely aligns with the

floating potential. Tight coupling of the inductors to the tip prevents RF oscillations and minimizes stray capacitance. The presence of stray capacitance effectively cuts off the impact of the inductors. During data acquisition, the probe tip is DC-biased through an electrical filter. The data-gathering device is equipped with a built-in microcontroller featuring a (16-Bit-33 MHz CPU, 4k on-chip SRAM memory, and 128k on-chip) ROM. Figure 3.4 illustrates the RF-compensated probe employed in the study.

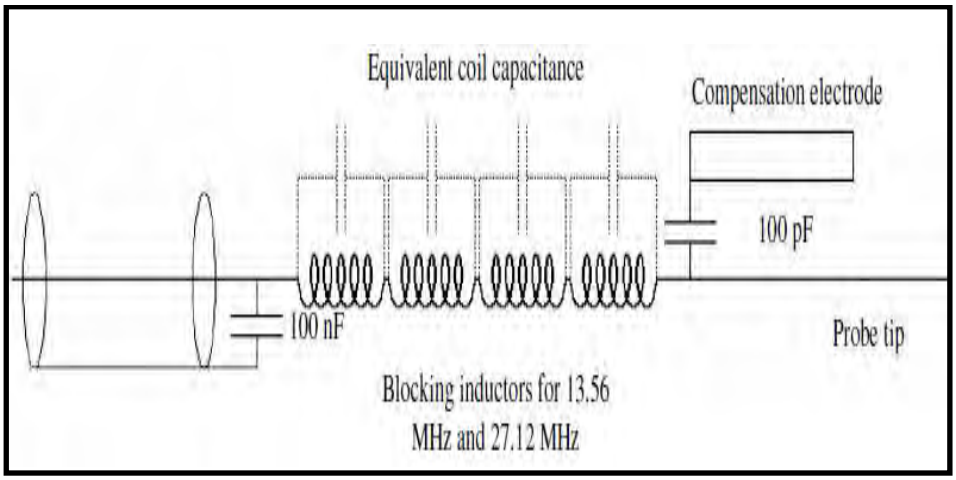

Figure 3. 4**:** A passive RF compensation circuit of LP.

3.4 Reference Electrode

The Smart Probe unit includes a floating reference electrode set at the plasma potential to account for potential variations in the probe. Adding potential to the probe induces a DC shift in the plasma potential due to the discharge's resistance to the sheath. To mitigate low-frequency noise in the plasma potential, a reference electrode is utilized.

While diagnosing laboratory plasma, surface contamination of the probe occurs due to working gases and chemical interactions between plasma species and probe material. This contamination forms a thick layer of deposition around the probe's surface, leading to poor probe operation and the development of a low-conductivity layer, which adds resistance to the probe circuit. Consequently, the I-V characteristic curve becomes erroneous, and issues such as photoemission of secondary electrons and ions may arise, potentially distorting the Electron Energy Probability Function (EEPF), particularly in the low-energy region. Probe surface contamination can also result in an extremely high electron temperature or hysteresis in the I-V curve [63].

Probe contamination is typically addressed through two methods: electron heating or ion bombardment. In electron heating, the probe is given a strong positive potential to draw a significant electron current and heat the tip, removing the deposited coating. Alternatively, in ion bombardment, the probe tip is negatively biased, attracting ions during collision and stripping the resistive coating. The Smart Probe system features both manual and automatic cleaning capabilities, measuring power to the probe tip while adjusting the pulse biasing voltage from 10 to 100 V during the cleaning procedure.

The system has automatic self-correction mechanisms for environmental changes like variations in pressure and power, but substantial deposit layers can render this function ineffective. This occurs when the applied voltage equals or slightly exceeds the plasma potential at a plasma density of $10^{12} cm^{-3}$ in low-density plasma (5 x 10^{7} to 5 x $10^{8} cm^{-3}$).

CHAPTER 04

RESULTS AND DISCUSSION

In this chapter the behavior of different physical parameters of Argon plasma generated by Magnetic Pole-Enhanced Inductively Coupled (MaPE-IC) system is presented. Different plasma parameters i.e. electron density (n_e), electron temperature (T_e), plasma potential (V_p) and Electron Energy Probability Function (EEPF) in low pressure regime are studied with variation in probe length.

4.1 Introduction

In the experiment, argon plasma is generated in MaPE-IC system at 1 Pa, 5 Pa and 10 Pa with RF power varied from 5 watt to 100 watt with increment of 5 watt. Respectively single Langmuir probe system with control circuit is used to measured different plasma parameters, such as electron density (n_e), electron temperature (T_e), plasma potential (V_p) and electron energy probability function (EEPF). Different probe lengths are used for measurement of above plasma parameters. The behavior of these parameters is discussed as under.

4.2 Electron Density (n_e)

Figures 4.1 (a), 4.1 (b), and 4.1 (c) expressed the behavior of electron density with probe length variation at a constant pressure of 1 Pa, 5 Pa, and 10 Pa while RF power is varied. It shows that at constant pressure and RF power, when probe length increases the electron density enhances. It is evident that the probe collects more and more electrons from the plasma which is why the electron current to the circuit increases [64].

From figures 4.1 (a), 4.1 (b), and 4.1 (c) it is also clear that the electron density increases with the enhancement of RF power at constant pressure. It may be due to the fact when RF power increases, low-energy electrons gain more and more energy from the external electromagnetic field. During the inelastic collision of these high-energy electrons with neutrals atoms, it excites/ionizes the neutrals atoms, consequently the electron density increases with RF power [68].

It is also evident from this figures 4.1 (a), 4.1 (b), and 4.1 (c) that the electron density increases with pressure variation at fixed RF power. The reason is that, with the increase of pressure atomic density increases per unit volume, as a results rate of collision of

electrons with neutral atoms also enhances, consequently electron density increases with increase of pressure.

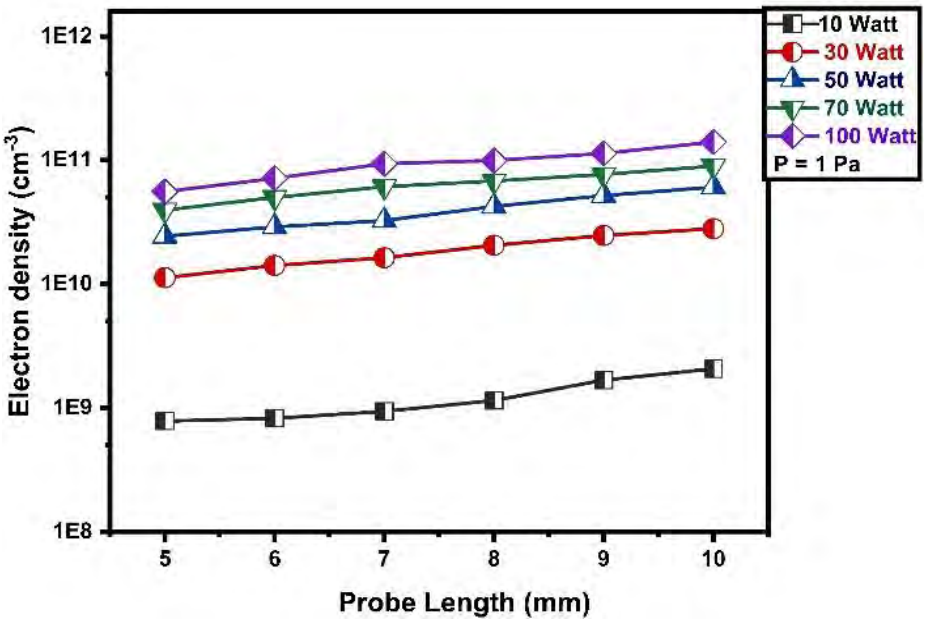

Figure 4.1**(a):** Graph between probe length and electron density (n_e) at 1 Pa with varying RF power.

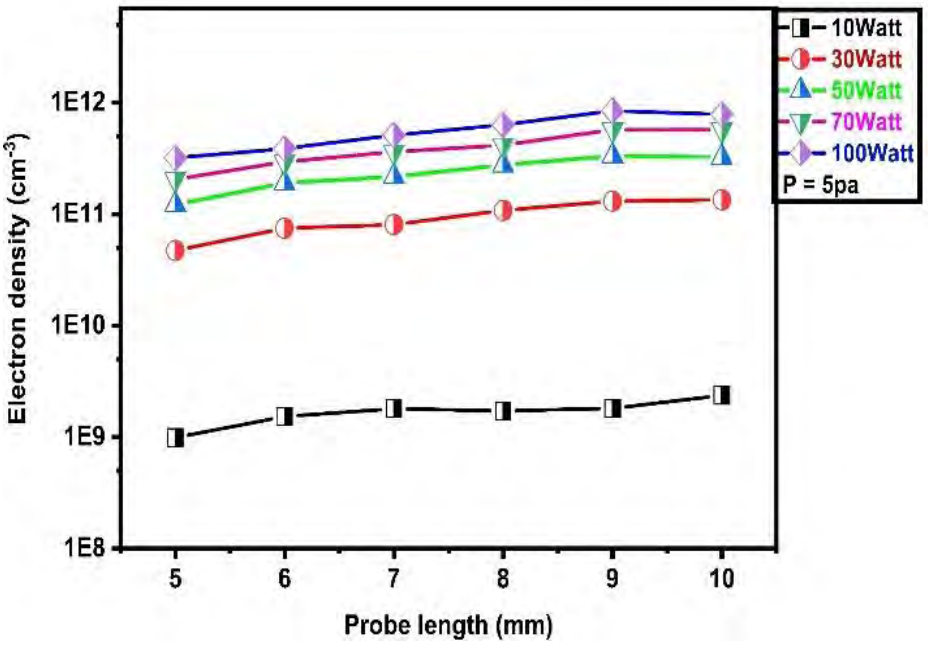

Figure 4.1 **(b):** Graph between probe length and electron density (n_e) at 5 Pa with varying RF power.

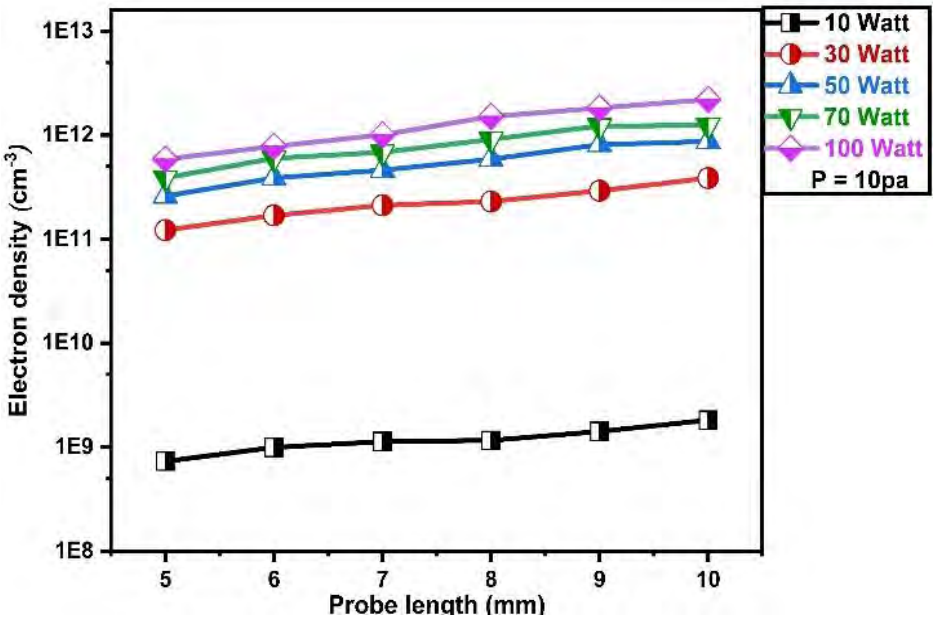

Figure 4.1 **(c):** Graph between probe length and electron density (n_e) at 10 Pa with varying RF power.

4.3 Electron Temperature (T_e)

Figures 4.2 (a), 4.2 (b), and 4.2 (c) describe the behavior of electron temperature with the variation of probe lengths at constant pressure and RF power. A slight decrease in electron temperature is recorded with the increase in probe length. It is because the high-energy electrons involve in inelastic collision with neutral atoms lose their energies. So, the electrons collected by the probe have small average energy [66].

Figures 4.2 (a), 4.2 (b), and 4.2 (c) also shows that at low RF power, the electron temperature is greater as compared to a higher power. It may be because that at low power, electrons have insufficient energy to involve in the excitation/ionization processes of neutral atoms and continuously gain energy from the external electromagnetic field. However, when RF power increases the electrons absorbs sufficient energy from external field and instigate ionization process. Resultantly, electron temperature decreases e RF power at constant pressure [67].

These graphs also expressed that electron temperature shows decreasing trend with increase in pressure at constant RF power. The number of collisions of energetic electrons with

neutral atoms increases, consequently electron losses energy. Therefore, the average energy of electrons decreases [68].

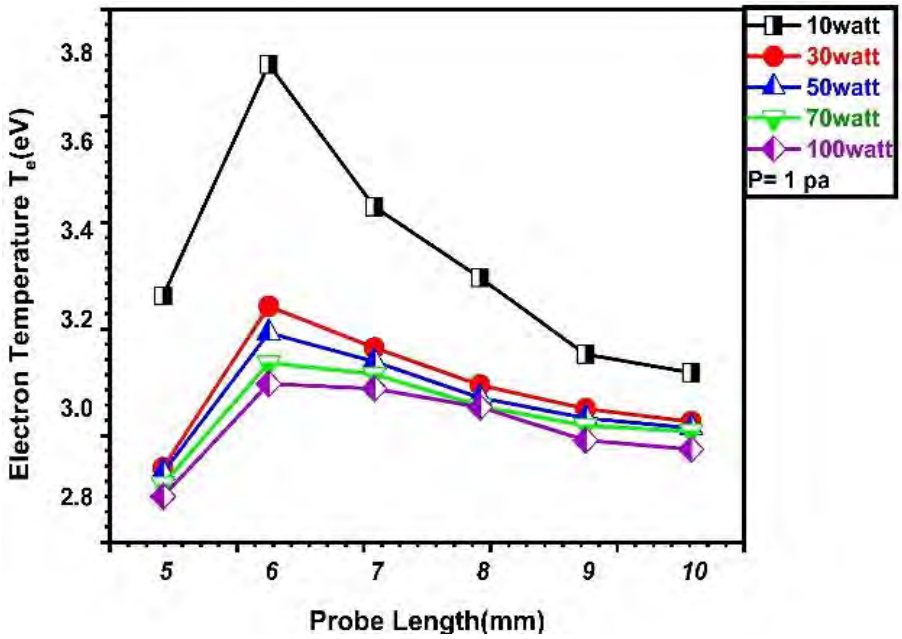

Figure 4.2 **(a):** Graph between probe length and electron temperature (T_e) at 1 Pa with varying RF power.

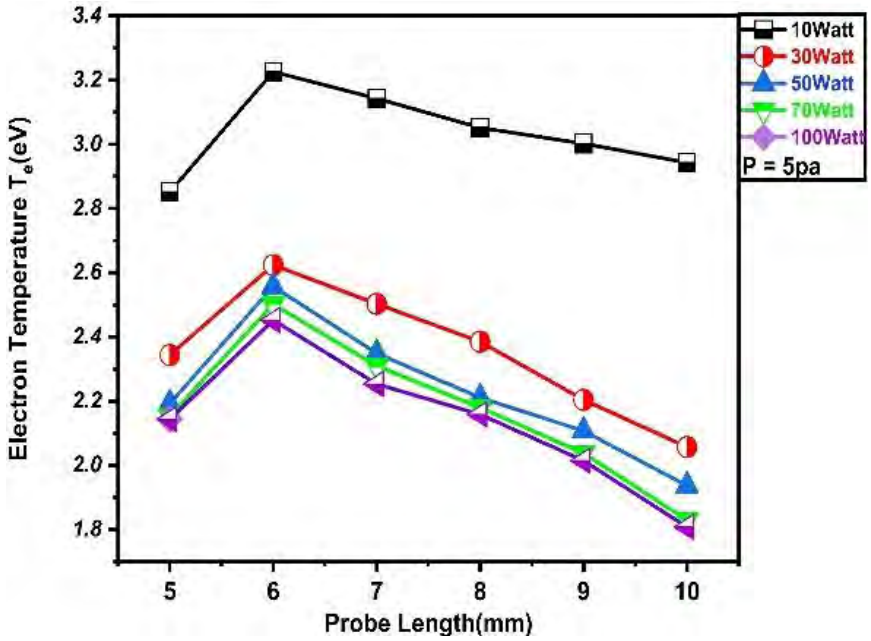

Figure 4.2 **(b):** Graph between probe length and electron temperature (T_e) at 5 Pa with varying RF power.

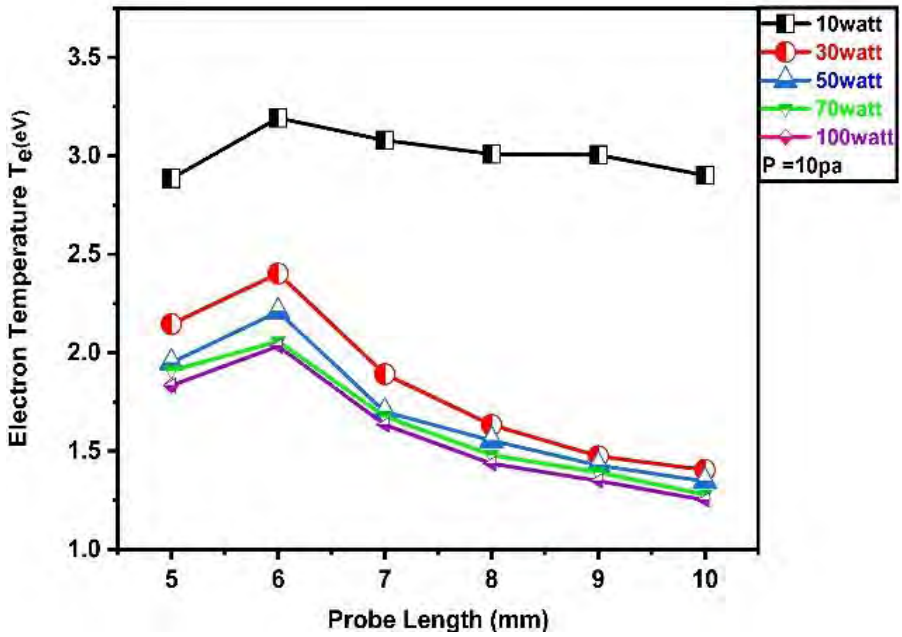

Figure 4.2 **(c):** Graph between probe length and electron temperature (T_e) at 10 Pa with varying RF power.

4.4 Plasma Potential (Vp)

The plasma potential "Vp" is a significant parameter of plasma that manages the ion energies in the sheath region. Any variations in Vp, determine the E-field that delivers energy to the free electrons to continue ionization processes within the plasma. The change in plasma potential with increasing RF power is represented in figures 4.3 (a), 4.3 (b), and 4.3 (c). At low pressure of 1 Pa as shown in Figures 4.2 (a) the plasma potential increases while at higher pressure (5 Pa and 10 Pa) constant behavior of plasma potential is observed. At low pressure, the increase in plasma potential indicates the occurrence of a slighter number of electrons in the bulk of plasma owing to the little rate of ionization at a smaller RF power and the high energy electron diffusion towards the reactor walls. Therefore, a small amount of electron reaches the probe and resultantly plasma potential shows an increasing trend with probe length. At all pressures (1 Pa, 5 Pa, and 10 Pa) with RF power, the plasma potential exhibits increasing behavior. It is because at low RF power the rate of ionization is weak and high energy electron escape towards the wall.

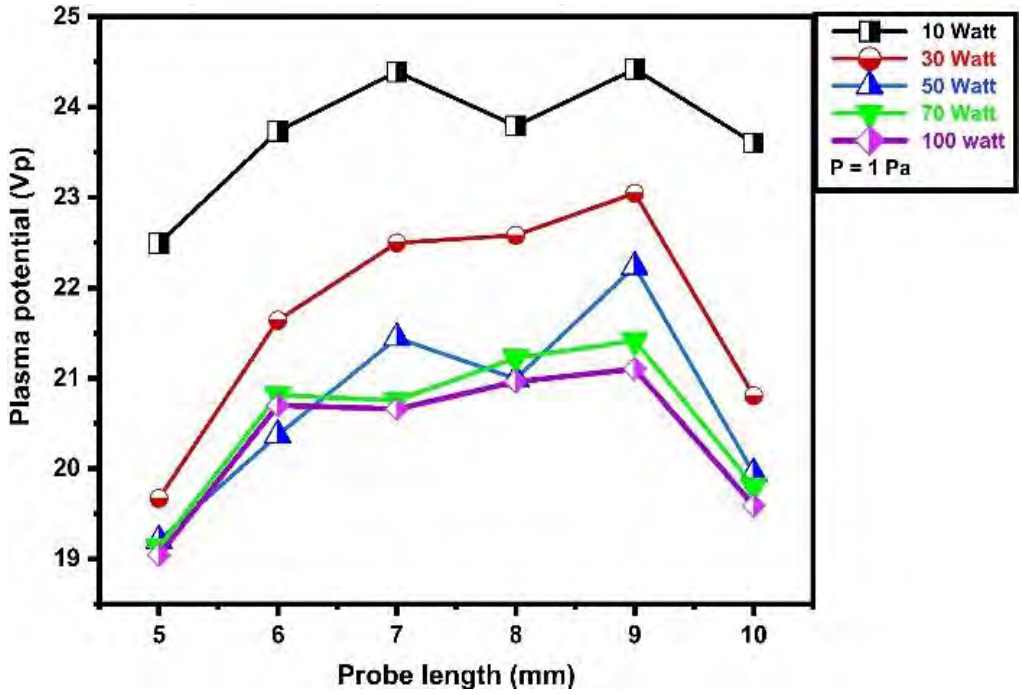

Figure 4.3 **(a):** Graph between plasma potential (v_p) and probe length at 1 Pa with varying RF power.

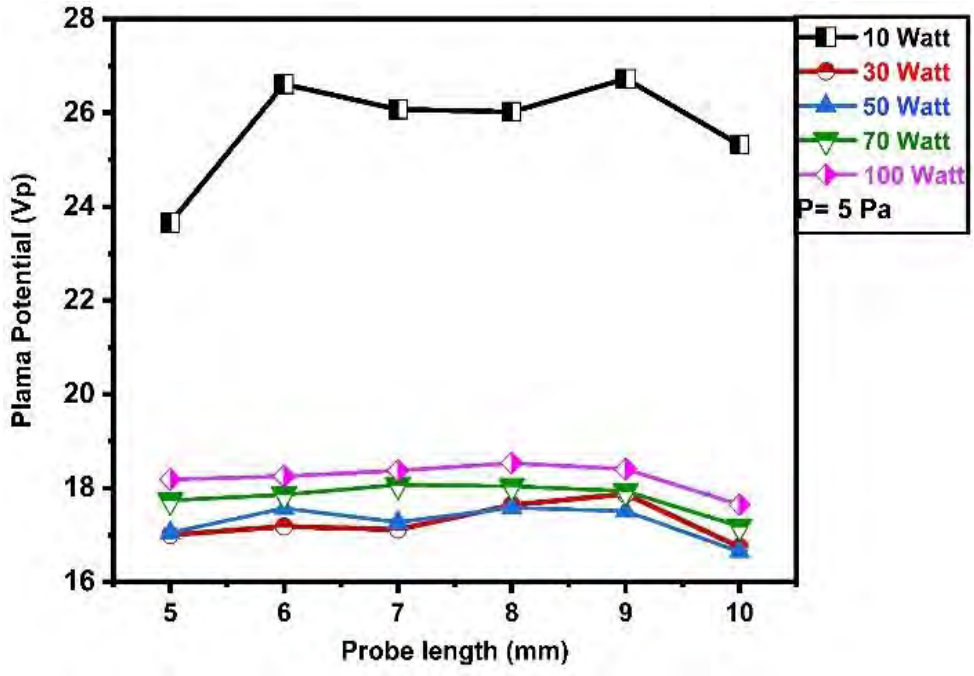

Figure 4.3 **(b):** Graph between plasma potential (v_p) and probe length at 5 Pa with varying RF power.

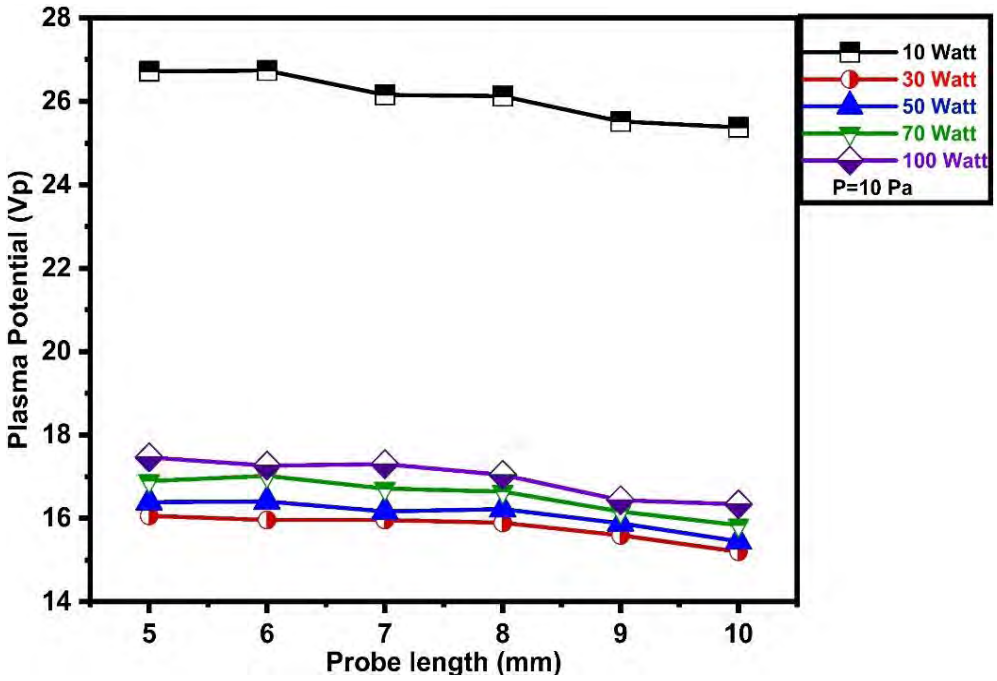

Figure 4.3 **(c):** Graph between plasma potential (v_p) and probe length at 10 Pa with varying RF power.

4.5 Evaluation of electron energy probability functions (EEPFs)

The determined EEPFs profiles for Langmuir probe length at a fixed pressure of 1 Pa, 5 Pa and 10 Pa while RF power 30W, 60W, and 100W are shown in figures 4.4 (a), 4.4 (b), 4.4 (c), 4.4 (d), 4.4 (e), 4.4 (f) and 4.4 (g). At low gas pressures and with applied RF powers, the EEPF exhibits a bi-Maxwellian distribution, which is a typical characteristic of non-local electron kinetics [13]. The bi-Maxwellian EEPF is a result of electron sheath heating without collision. As a result, the population of tail electrons increases, and the population of electrons in the 2-4 eV region, where vibrational excitations take place, decreases. As a result, the EEPF profile shows a dip near the resonant vibrational excitations.

The following can be used to explain how the distribution function has evolved. Because the frequency of electron-neutral collisions is substantially lower at low pressure and RF power than the applied RF frequency, the electromagnetic field penetration associated with the RF frequency results in collision less heating of the electrons. High-energy electrons have the cane DC ambipolar potential and enter the sheath area, where they are efficiently heated by the collision less method.

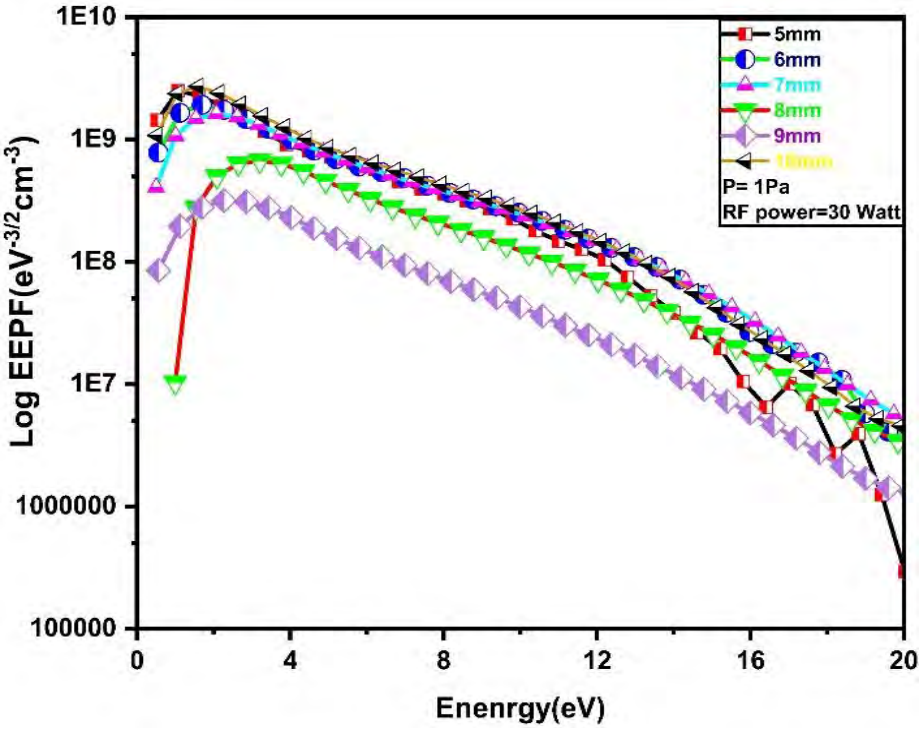

Figure 4.4 **(a):** Graph between EEPF and Energy at 1 Pa and 30 Watt RF power.

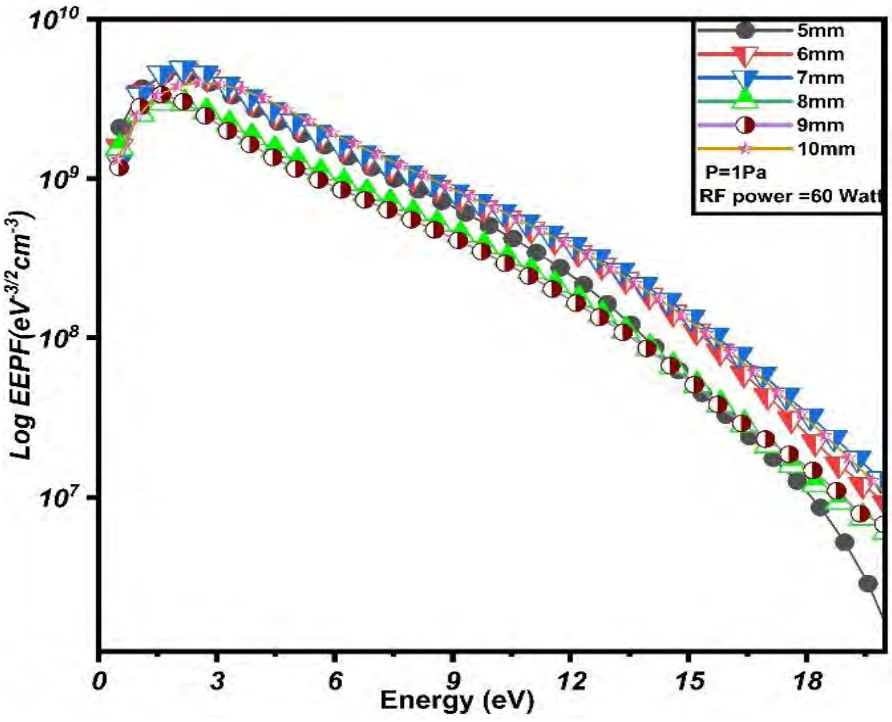

Figure 4.4 **(b):** Graph between EEPF and Energy at 1 Pa and 60 Watt RF power.

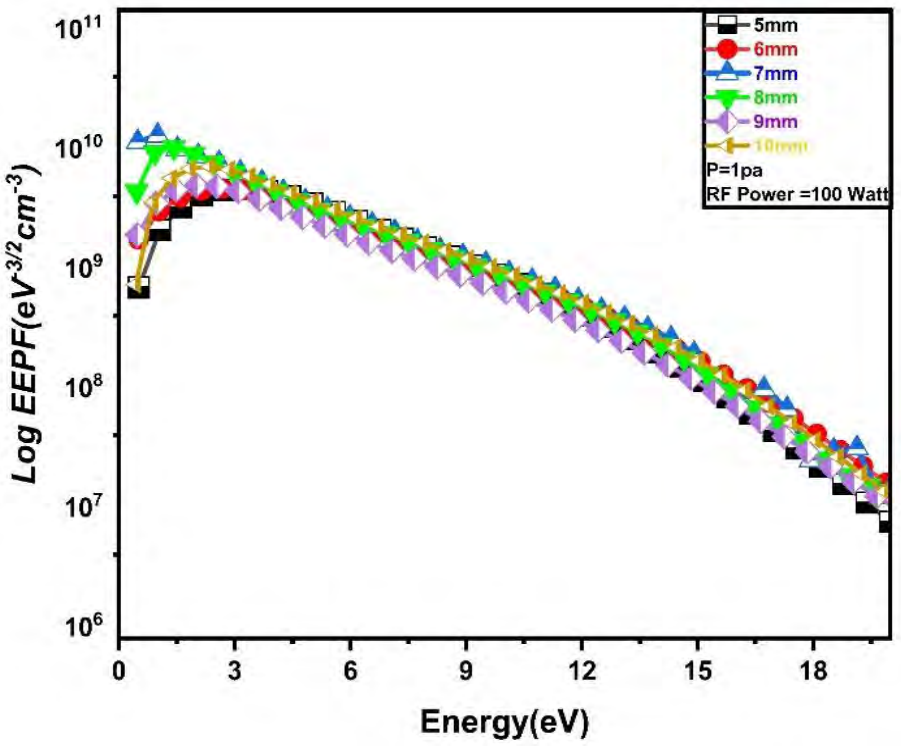

Figure 4.4 **(c):** Graph between EEPF and Energy at 1 Pa and 100 Watt RF power.

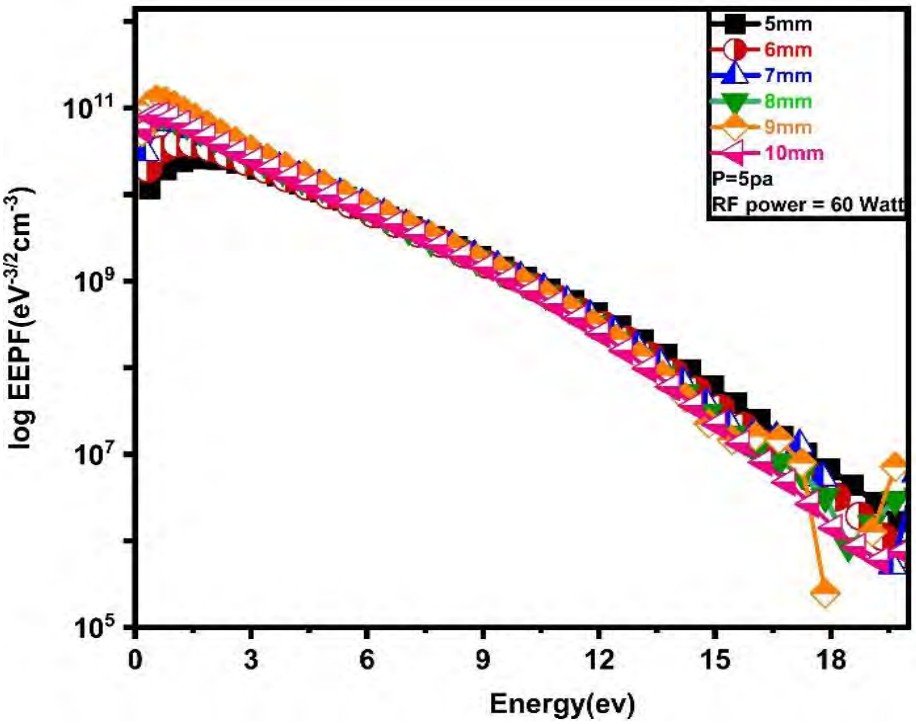

Figure 4.4 **(d):** Graph between EEPF and Energy at 5 Pa and 60 Watt RF power.

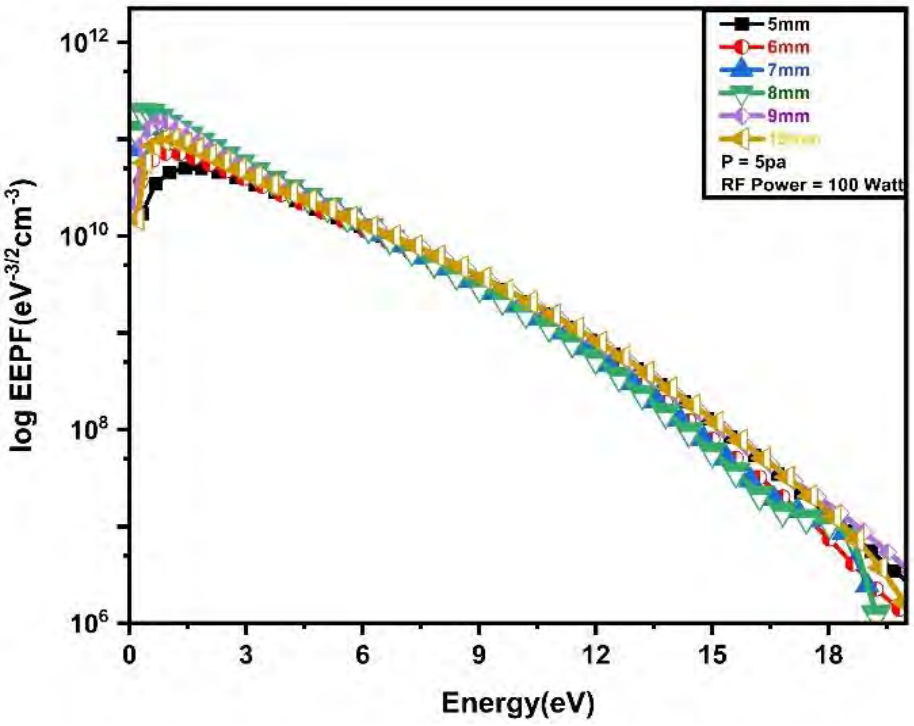

Figure 4.4 **(e):** Graph between EEPF and Energy at 5 Pa and 100 Watt RF power.

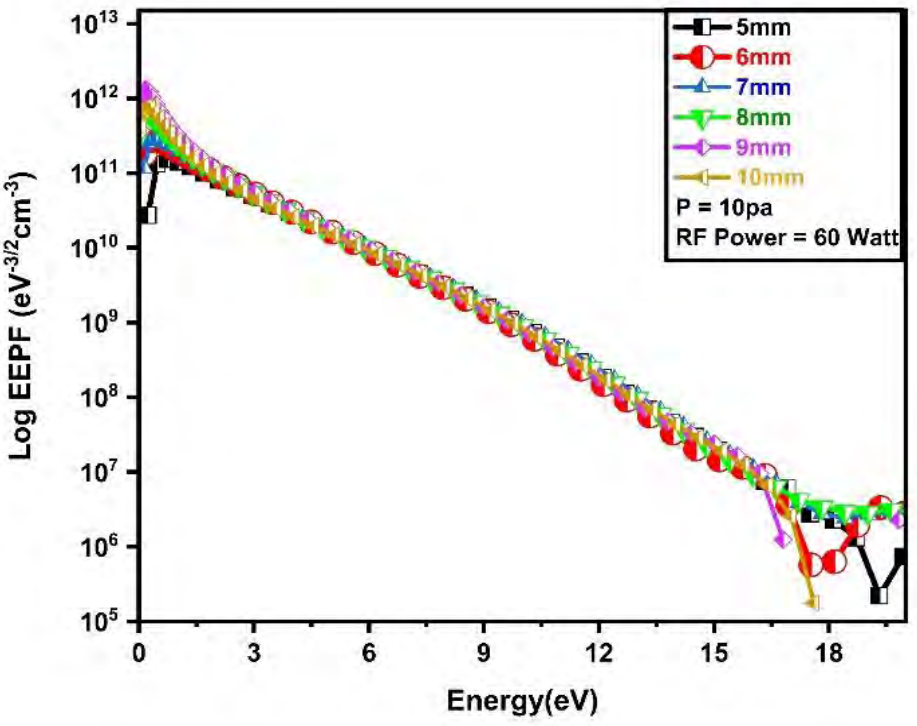

Figure 4.4 **(f):** Graph between EEPF and Energy at 10 Pa and 60 Watt RF power.

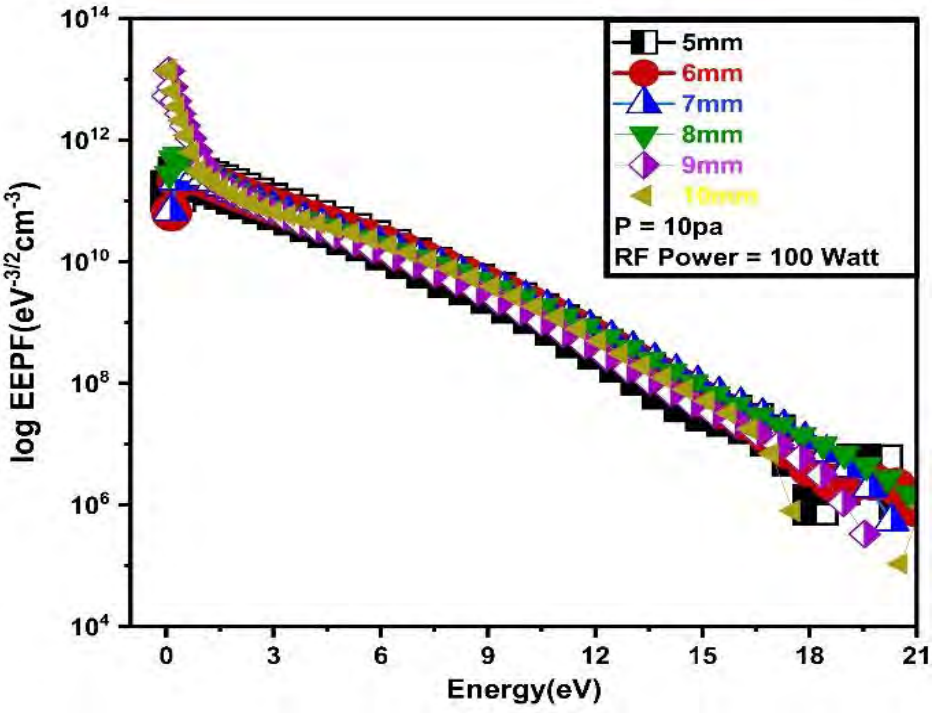

Figure 4.4 **(g):** Graph between EEPF and Energy at 10 Pa and 100 Watt RF power.

The ionization and excitation processes are caused by the heated electrons' participation in numerous inelastic collisions. The low-energy electrons, on the other hand, are heated by collisions and remain trapped in the bulk. Due to low collisional frequency and a weaker electric field in the bulk, collisional heating is typically ineffective at low pressures. As a result, they merely oscillate in the ambipolar potential and do not generate much energy through any heating mechanism.

Furthermore, the changes in various energy transport pathways (gain and loss) in the plasma are related to the evolution of EEPF profiles with the addition of the mixture. First off, high-energy electrons can be produced through super-elastic collisions between electrons in addition to inelastic collisions between electrons and nitrogen molecules [69]. Due to the being unable to overcome the ambipolar potential, there are two different groups of electrons: the high-energy group and the low-energy group. As a result, the bi-Maxwellian electron distribution is seen at low RF powers. EEPFs change from a bi-Maxwellian to a Maxwellian distribution when RF power increases (over 50 W), but an increase in one tends to diminish the electrostatic heating of electrons due to high electron-electron collision frequency.

4.6 Conclusions

In this research work the behavior of basic Argon plasma parameters with probe length variation at constant pressure and RF power are investigated by using RF compensated Langmuir Probe.

At constant pressure and RF power, the high electron density is recorded by the probe having a greater length. It is found that electron density increases with probe length at fixed RF power and Pressure. At a single probe length, the electron density shows an increasing trend with RF power at constant pressure. Small decrease in electron temperature is observed with probe length at constant pressure and RF power. Plasma potential expressed nearly constant behavior with probe length at constant pressure and RF power. In EEPF, no such variation is observed with probe length.

4.7 Suggestion for Future Work

Langmuir probe is one of the main diagnostic tools used for the investigation of different types of plasma. The effect of probe tip diameter on different argon plasma parameters should be investigated. The results of this research could help improve the accuracy of Langmuir probe measurements and provide insight into the behavior of plasma.

References

[1] D. Macauley, “Elemental Philosophy, Earth, air, water and fire as fundamental ideas” Suny Press 2010,

[2] Robert J. Goldston and Paul H. Rutherford “Introduction to plasma physics” Plasma Physics laboratory Princeton University 1995 IOP Published ltd.

[3] S. Samal “Thermal Plasma Processing of Ilmenite” Springer 2017.

[4] F. F. Chen, "Introduction to plasma physics and controlled fusion", Springer, 1984.

[5] Piel, Plasma Physics: An Introduction to Laboratory, Space, and Fusion Plasmas, London New York: Springer, 2010.

[6] D. L. Conde, "An Introduction to Plasma Physics and its Space Applications," 2014.

[7] L. A. Kennedy et. al. "Plasma physics and engineering", Taylor & Francis, 2004.

[8] H. Rauscher et. al. "Plasma technology for hyper-functional surfaces: food, biomedical and textile applications", John Wiley & Sons, 2010.

[9] B. M. Smirnov, "Physics of ionized gases", John Wiley & Sons, 2008.

[10] Y. P. Raizer, "Radio-frequency capacitive discharges", CRC Press,

[11] Fridman, "Plasma medicine", John Wiley & Sons, 2012. 2017.

[12] F. Penning, Über ionization durch metastable atom, Naturwissenschaften, 15 (1927) 818-818.

[13] J. Franklin, "Ton-molecule reactions", Springer Science & Business Media, 2012

[14] K. S. Harsha, "Principles of vapor deposition of thin films", Elsevier, 2005.

[15] D. M. Mattox, "Handbook of physical vapor deposition (PVD) processing", William Andrew, 2010

[16] Shimamura, et. al. "Electron-molecule collisions", Springer Science & Business Media, 2013.

[17] B. M. Smirnov, Reference data on atomic physics and atomic processes, Springer Science & Business Media, 2008.

[18] Fridman, Plasma Chemistry, Cambridge University Press, 2008.

[19] M. A. Lieberman et. al. "Principles of plasma discharges and materials processing", John Wiley & Sons, 2005.

[20] F. F. Chen, et. al. "Lecture notes on principles of plasma processing", Springer Science & Business Media, 2012.

[21] Plasma Physics and Engineering CRC 2004.

[22] V. A. Godyak, R. Piejak and B. Alexandrovich, Measurement of electron energy distribution in low-pressure RF discharges. Plasma Sources Sci. Technol. 1 (1992) 36.

[23] Y. P. Raizer., Gas Discharge Physics, Springer-Verlag, 1997.

[24] M.J.Druyvesteynn, Der Niedervoltbogen, vol. 64, Zeitschrift für Physik, 1930.

[25] H. Griem ‘’Principles of plasma Spectroscopy,’’ Cambridge University Press, 1997.

[26] Y.T.T. Sakuta ‘Plasma Sources Science Technology’, vol. 12, 2003.

[27] Thorne, Spectrophysics, Springer Netherlands, (2012).

[28] Gleizes, A., J.-J. Gonzalez, and P. Freton, Thermal plasma modelling. Journal of Physics D: Applied Physics, 2005. 38(9): p. R153.

[29] X. M. Zhu and Y. K. Pu, Optical emission spectroscopy in low-temperature plasmas containing argon and nitrogen: determination of the electron temperature and density by the line-ratio method, J. Phys. D: Applied Phys. 43 (2010) 403001.

[30] Grill, A., Cold plasma in materials fabrication. Vol. 151. 1994: IEEE Press, New York.

[31] Marcel Goosens. An Introduction to Plasma Astrophysics and Magneto thermodynamics (2003).

[32] R. L. Merlino, Understanding Langmuir probe current-voltage characteristics, Am. J. Phys. 75 (2007) 1078.

[33] J. Allen, Probe theory-the orbital motion approach, Phys. Sci. 45 (1992) 497.

[34] J. Allen, R. Boyd, and P. Reynolds, The collection of positive ions by a probe immersed in a plasma. Proceedings of the Physical Society. Section B 70 (1957) 297.

[35] V. Godyak, Steady-state low-pressure rf discharge, Sov. J. Plasma Phys. 2 (1976) 78.

[36] P. Chabert, ET. al. "Physics of radio-frequency plasmas", Cambridge University.

[37] M. Zaka-ul-Islam, "A study of electron dynamics in a single and dual frequency inductively coupled plasma system", Queen's University Belfast, 2012.

[38] P. Chabert, N. Braithwaite, Physics of radio-frequency plasmas, Cambridge University Press, 2011.

[39] G. Cunge, et. al. "Characterization of the E to H transition in a pulsed inductively coupled plasma discharge with internal coll geometry: bi-stability and hysteresis", Plasma Sources Science and Technology, 8 (1999) 576.

[40] M. Turner and M. Lieberman, Hysteresis and the E-to-H transition in radiofrequency inductive discharges, Plasma Sources Sci. Technol. 8 (1999) 313.

[41] M. Turner, "Collisionless electron heating in an inductively coupled discharge", Physical review letters, 71 (1993) 1844.

[42] El-Fayoumi, I. Jones and M. Turner, Hysteresis in the E-to H-mode transition in a planar coil, inductively coupled rf argon discharge, J. Phys. D: Appl. Phys. 31 (1998) 3082.

[43] U. Kortshagen, et. al. "On the E-H mode transition in RF inductive discharges", Journal of Physics D: Applied Physics, 29 (1996) 1224.

[44] R. P. Chang, "Plasma oxidation of semiconductor and metal surfaces, in Passivity of Metals and Semiconductors", Elsevier, 1983, pp. 437-444.

[45] https://tuttnauer.com/blog/low-temperature-hydrogen-peroxide-plasma-

[46] https://en.wikipedia.org/wiki/Plasma-enhanced_chemical_vapor_deposition.

[47] M. A. Morshed, "Application of Plasma Technology in Textile: A Nanoscale Finishing Process".

[48] Bogaerts, et al., Plasma diagnostics of an analytical Grimm-type glow discharge in argon and in neon: Langmuir probe and optical emission spectrometry measurements, Spectrochim. Acta Part B 50 (1995) 1337.

[49] M. Hopkins, Langmuir probe measurements in the gaseous electronics conference RF reference cell, J. Res. Natl. Stand. Technol. 100 (1995) 415.

[50] A Thorne, Spectrophysics, Springer Netherlands, (2012).

[51] U. Fantz, Basics of plasma spectroscopy, Plasma Sources Sci. Technol. 15 (2006) SI37.

[52] G. González, F. Gonzalez, A new approach to the Child-Langmuir law, arXiv preprint arXiv: 1506.07417, (2015).

[53] Langmuir and H. Mott-Smith, Studies of electric discharges in gases at low-pressure part II-typical experimental data illustrating the use of plane collectors, Gen. Elec. Rev. 27 (1924) 538.

[54] H. M. Mott-Smith and I. Langmuir, The theory of collectors in gaseous discharges, Phys. Rev. 28 (1926) 727.

[55] R. L. Merlino, Understanding Langmuir probe current-voltage characteristics, Am. J. Phys. 75 (2007) 1078.

[56] F. F. Chen, J. D. Evans and W. Zawislak. Electric probes. In Plasma Diagnostic Techniques, Ed. R. H. Huddlestone, and S. L. Leonard, Citeseer (1965)

[57] W. Khan, Investigation of Plasma Parameters and Active Species Concentration in RF Excited Low Temperature Plasmas, in, Gomal University, DI Khan., 2018.

[58] H. Amemiya, Plasmas with negative ions-probe measurements and charge equilibrium, Journal of Physics D: Applied Physics, 23 (1990) 999.

[59] J.D Swift and M. Schwar, Electrical probe for plasma Diagnostics, (1970)

[60] O. Auciello, et al., Plasma-Surface Interactions and Processing of Materials, Springer Netherlands, (2012).

[61] Investigations of Capacitively-Coupled Plasmas by Electrostatic Probe Technique

[62] U. Flender, B.N. Thi, K. Wiesemann, N. Khromov, N. Kolokolov, "RF harmonic suppression in Langmuir probe measurements in RF discharges", Plasma Sources Science and Technology, 5 (1996) 61.

[63] V. Godyak, R. Piejak, B. Alexandrovich, "Observation of second harmonic currents in inductively coupled plasmas", Physical Review Letters, 83 (1999) 1610.

[64] S. H. Seo et. al. On the heating mode transition in high-frequency inductively coupled argon discharge. Phys. Plasmas 6 (1999) 614.

[65] J. Hopwood, Ion bombardment energy distributions in a radio frequency induction plasma. Appl. Phys. Lett. 62 (1993) 940.

[66] T. Kimura and H. Kasugai, Experiments and global model of inductively coupled rf Ar/N, discharges. J. Appl. Phys. 108 (2010) 033305.

[67] K. Ishikawa et al., Surface reactions during etching of organic low-k films by plasmas of N2 and H2. J. Appl. Phys. 99 (2006) 083305.

[68] T. Czerwiec, F. Greer and D. Graves, Nitrogen dissociation in a low pressure cylindrical ICP discharge studied by actinometrical and mass spectrometry. J. Phys. D: Appl. Phys. 38 (2005) 4278.

[69] K. Zheng-De and P. Yi-Kang, Electron temperature control in inductively coupled nitrogen plasmas by adding argon/helium. Chin. Phys. Lett. 19 (2002) 1139.